# Basic Principles of Cryotropic Gelation

**Vladimir I. Lozinsky and Oguz Okay**

## Contents

1 Introduction ..... 50
1.1 "Gels" in General, and "Cryogels" in Particular ..... 51
1.2 "Cryotropic Gelation" ..... 51
1.3 "Positive" and "Negative" Temperature ..... 51
1.4 "Gel-Fraction" and "Gel-Fraction Yield" ..... 52
2 Main Stages of the Cryotropic Gelation Processes ..... 52
2.1 Preparation of the Feed System ..... 53
2.2 Freezing of the Feed ..... 54
2.3 Incubation of the Gelation System in a Frozen State ..... 58
2.4 Thawing of the Frozen System ..... 60
3 Specific Effects of Gel Formation in Moderately Frozen Systems ..... 66
3.1 Apparent Decrease in the Critical Concentration of Gelation ..... 66
3.2 Acceleration of Gel Formation Over a Certain Range of Negative Temperatures . . 73
3.3 Bell-Shaped Temperature Dependence of Cryotropic Gelation Efficiency ..... 78
3.4 Generation of Specific Porosity Peculiar to Cryogels ..... 84
4 Conclusions ..... 95
References ..... 96

**Abstract** Polymeric cryogels are the gel systems formed in moderately frozen solutions or colloidal dispersions of precursors potentially capable of gelling. Polymeric cryogels are of growing practical interest in various applied areas. The fabrication of any cryogel includes the following necessary stages: preparation of the feed system, its freezing, incubation of the gelation system in a frozen state, and

V.I. Lozinsky (✉)
Laboratory for Cryochemistry of (Bio)Polymers, A.N. Nesmeyanov Institute of Organoelement Compounds, Russian Academy of Sciences, Vavilov Street 28, 119991 Moscow, Russian Federation
e-mail: loz@ineos.ac.ru

O. Okay
Department of Chemistry, Istanbul Technical University, Maslak, 34469 Istanbul, Turkey
e-mail: okayo@itu.edu.tr

O. Okay (ed.), *Polymeric Cryogels*, Advances in Polymer Science 263,
DOI 10.1007/978-3-319-05846-7_2, © Springer International Publishing Switzerland 2014

thawing of the frozen sample. The nature of gel precursors, their concentration in the initial feed, and the conditions of each of the stages affect the physicochemical properties and porous morphology of the resulting cryogels. Certain specific effects are inherent in the processes of cryotropic gel formation, namely, apparent decrease in the critical concentration of gelation, acceleration of gel formation over a certain range of negative temperatures, a bell-shaped temperature dependence of the cryotropic gelation efficiency, and generation of the specific porosity peculiar to cryogels. This chapter presents the basic principles of cryotropic gelation processes and also discusses the factors influencing the properties of various types of cryogels.

**Keywords** Cryotropic gelation • Unfrozen liquid microphase • Freezing • Frozen storage • Defrosting

## Abbreviations

| | |
|---|---|
| CCG | Critical concentration of gelation |
| CTAB | Cetyltrimethylammonium bromide |
| DMSO | Dimethylsulfoxide |
| GuAr | Gum arabic |
| LCST | Lower critical solution temperature |
| NMR | Nuclear magnetic resonance |
| PVA | Poly(vinyl alcohol) |
| SEM | Scanning electron microscopy |
| UCST | Upper critical solution temperature |
| UFLMP | Unfrozen liquid microphase |
| VA | Vinyl alcohol |
| VAc | Vinyl acetate |

## 1 Introduction

As described in the previous chapter of this volume [1], studies on the gel formation processes in moderately frozen solutions or colloidal dispersions containing the necessary precursors started at the beginning of 1970s, although empirical observations of freeze–thaw-caused gelation were made long before. The experimental data obtained during the past four decades in this field have resulted in a sum of knowledge on the general aspects of cryotropic gelation, which is the subject of the present chapter. Before starting the discussion, the terminology will be defined in order to clarify what each specialized term means.

## 1.1 "Gels" in General, and "Cryogels" in Particular

There are many definitions of what the gels are [2–6], and some of these definitions are rather complicated because they include numerous significant properties of the polymeric systems classified as gels. However, at a qualitative level one can say that gels are systems consisting of polymer and immobilized solvent in which macromolecular chains are connected to each other via chemical or physical bonds, forming a 3D network. The definition can be made simpler still: gels are swollen spatial polymeric networks. If the immobilized solvent is water, then we deal with hydrogels; if the solvent is an organic liquid, then organogels are considered. Certainly, various intermediate variants are also possible when the solvents are water–organic mixtures. Depending on the nature of the interchain bonds in the nodes of the polymeric 3D network, gels are commonly classified as follows: covalent (i.e., chemically crosslinked) gels; ionically or ion-chelately crosslinked gels; and noncovalent or physical gels. "Mixed" variants also exist. The gel's bulk morphology (homophase or heterophase) is determined by the chemical structure of the constituent polymers and by the method of gel preparation. In this context, cryogels are gel systems whose formation occurs in moderately frozen solutions or colloidal dispersions of precursors potentially capable of gelling [7, 8]. Therefore, the occurrence of gel formation in the frozen precursor-containing system is the necessary specific feature that distinguishes cryotropic gelation from gel formation at temperatures above the freezing point of the feed [9].

## 1.2 "Cryotropic Gelation"

The word combination "cryotropic gelation" connects directly with the proper processes resulting in the formation of diverse cryogels. The term's construction is similar to that of the terms "chemotropic" (caused by chemical reactions), "ionotropic" (caused by ionic bonding), and thermotropic gel formation (caused by heating, as in the gelation of aqueous solutions of methylcellulose upon warming above the lower critical solution temperature, LCST). Hence, cryotropic gelation, derived from the Greek *kryos* (frost) and *tropos* (cause), is gel formation caused by the cryogenic treatment (freezing–frozen storage–thawing) of the precursor system. The solvent crystallization in this process acts as a trigger enabling the subsequent gelation phenomena.

## 1.3 "Positive" and "Negative" Temperature

These terms are defined as, respectively, the temperatures above and below the freezing/melting point of the initially liquid system (see [1]). In addition, in the course of further discussions on nonaqueous systems we will also operate, when

needed, with the relative temperature $\Delta T$, defined as $\Delta T = T_i - T_0$, where $T_0$ is the freezing point of the solvent used and $T_i$ is the gelation temperature. Thus, if gelation occurs in the medium of formamide ($T_0 = +2.9$ °C), $\Delta T = -20$ and +20 °C correspond to gelation temperatures $T_i$ of −17.1 and +22.9 °C, respectively. Similarly, for gelation in cycloheptane with $T_0 = -12$ °C, $\Delta T = -20$ and +20 °C correspond to $T_i = -32$ and +8 °C, respectively.

### *1.4 "Gel-Fraction" and "Gel-Fraction Yield"*

It is rather hard to measure experimentally with high precision the real content of the gel phase, that is, the amount of the separate system composed of the crosslinked polymer and immobilized solvent within the whole sample volume. This is particularly so for heterophase cryogels because the value measured will strongly depend on the swelling extent of the sample under a single set of examination conditions. That is why the notions "gel-fraction" and "gel-fraction yield" imply, although being insufficiently strict terminologically, the content or the yield of the dry crosslinked polymer relative to the dry weight of the respective precursors. Such a fraction is easily determined gravimetrically and does not depend on the swelling extent of the particular gel or cryogel samples. Besides, if the tightly bound solvate liquid is difficult to remove from the sample upon drying (as is frequently the case for hydrogels), the residual moisture amount can be quantified by auxiliary independent methods like Karl Fischer titration (e.g., see [10] for chitosan-based cryogels).

The goal of this chapter is to describe and discuss general aspects of cryotropic gelation with emphasis on its basic principles. The key factors affecting different stages of cryotropic gelation processes and, thus, influencing the properties and the structure of the resulting polymeric cryogels will also be considered. In addition, when the current knowledge level is sufficient, explanation will be given for the specific effects peculiar to this kind of gel formation.

## 2 Main Stages of the Cryotropic Gelation Processes

Similarly to the formation of conventional covalent gels, covalent cryogels are prepared either through the crosslinking polymerization or polycondensation of monomeric precursors, or by crosslinking (chemically or with radiation) of high molecular weight compounds, the latter being either in molecular-dissolved or in colloidal-dispersed forms [7, 8, 11]. In the case of noncovalent (physical) cryogels, the initial substances are usually polymers capable of self-gelling upon cooling of their solutions like water/gelatine [12] and poly(acrylonitrile)/*N*,*N*-dimethylformamide systems [13], or their colloidal dispersions like the gelatinized starch pastes [14, 15], or "cryosensitive" latexes [16, 17]. Ionic cryogels can, in principle,

be created from the solutions of polyelectrolytes by their crosslinking using counterions capable of forming low-dissociating ionic bonds between the charged groups of such macromolecular precursors [7, 8]. In all these cases, the procedure of cryogel preparation includes the following basic stages:

1. Preparation of the feed system
2. Freezing of the feed
3. Incubation of the system in a frozen state
4. Thawing of the frozen system

The conditions of each stage, including the properties of the particular precursors, affect more or less significantly the efficiency of cryotropic gel formation and, thus, the properties and structure of the resulting cryogel materials. So, it seems reasonable to discuss step-by-step the factors that are of importance for such freeze–thaw gelling systems.

## *2.1 Preparation of the Feed System*

At first sight, preparation of the initial feed containing the precursors of the future cryogel is a rather simple and routine procedure. This is a necessary step for the preparation of any gel material both at positive and negative temperatures. However, definite peculiarities of the cryotropic gel formation generally dictate certain requirements for the preparation of the initial system. For instance, one should minimize the conversion of the precursor to the gel before freezing the feed. Otherwise, if the gel-point is attained prior to the start of solvent crystallization, the destruction of the primary 3D network thus formed may occur by the creation of a polycrystalline phase. Such a process is especially detrimental in quickly forming chemotropic gels because their covalently linked nodes do not allow the polymeric chains to be slid apart easily by the growing solvent crystals. These effects, in turn, can even result in splitting of the weakest covalent bonds in the structure of the spatial polymeric network, especially, as shown by Jellinek and Fox [18], when the crystallization fronts are moving rapidly.

There are two ways to “outrun” gelation of the still-unfrozen feed system. The first method is to freeze the feed as quickly as possible where the gelation reactions have already begun. The other method is to reduce the initial rate of such reactions, e.g., by chilling the feed to just above its freezing point before adding the initiator (the case of polymerization-type cryogels) or the crosslinking agent (the case of covalent cryogels formed via crosslinking of macromolecular precursors). The former way, such as the flash-freezing technique using liquid nitrogen, has two significant drawbacks. First, the initial solution may undergo a glass-transition instead of the required solvent crystallization so that no cryo-concentration effect can be generated. Second, when the solvent crystallization does occur, the size of the very quickly formed crystals is small, and so is the cross-section of the pores in the resulting cryogel. Therefore, the latter approach, i.e., decreasing the rate of the

corresponding reactions prior to freezing of the feed, looks more promising. As a rule, for fast-reacting systems this goal is reached simply by chilling the initial feed. Some examples of the procedures employed for the preparation of polymerization-type cryogels and cryogels via chemical crosslinking of the polymeric precursors can be found in [19–25] and [10, 26–32], respectively.

The above considerations are mainly related to the preparation of covalent cryogels, where chilling the initial solution prior to the addition of either initiator or crosslinking agent does not lead to the gelation per se. However, when dealing with the preparation of physical cryogels, especially with systems undergoing a fast sol-to-gel transition at positive temperatures (such as aqueous agarose solutions), the situation is complicated. In such physically gelling systems one must decrease the self-gelation rate of the precursors to shift the gel-point to longer reaction times so that the gel will form within the volume of the unfrozen liquid microphase. As discussed in Sect. 2.4 of [1], the preferable way is to use specific solutes capable of slowing down gelation, e.g., alkaline additives for the preparation of wide-pore agarose cryogels [33, 34].

Moreover, the feed compositions capable of producing ionically crosslinked cryogels are even more sophisticated due to the very high rates of ionic reactions. Besides, such reactions are only slightly sensitive to the temperature. Therefore, cooling the initial feed containing dissolved polyelectolytes and necessary crosslinking counterions cannot sufficiently decelerate ionotropic gel formation prior to freezing of the system. Possible ways for bypassing such difficulties are also discussed in Sect. 2.5 of [1]. In short, in terms of the composition of the precursor solution, only two variants are relevant. The first method is to use a crosslinking agent with a negative temperature coefficient of solubility, e.g., solid salts exhibiting increased water solubility as the temperature is decreased [7, 8]. The second method, namely the so-called internal gelation approach, is to induce gelation via auxiliary agents capable of gradual solubilization of the dispersed salt particles containing crosslinking counterions [35, 36]. Whereas the former variant has already been realized in the preparation of Ca-alginate-based cryogels [37, 38], no cases of the implementation of the latter variant are known so far to the authors of this chapter.

## *2.2 Freezing of the Feed*

Freezing of the initial precursor-containing system is the crucial step for both the subsequent cryotropic gel formation per se and the properties of the resulting cryogels. This is due to several simultaneous processes that are launched during the transformation of the feed liquid into a frost-bound solid. These processes strongly alter the concentration and thermal mobility of the dissolved/dispersed gelation components, the volume of the unfrozen liquid fraction, its viscosity, and its polarity. Moreover, depending on the freezing conditions, they also influence the size and shape of the growing solvent polycrystals, thus biasing the macroporous

morphology of the resulting cryogels. In other words, freezing of the initial molecular or colloidal solution of the precursors affects not only the gelation efficiency, but also the structural characteristics of the final cryogel.

The key parameters of the freezing process are temperature, cooling rate, spontaneous or, if special procedures are employed, directed heat sink [39, 40], the ability of the initial liquid system to be supercooled, the presence of specially added or accidental (e.g., specks of dust) germs of crystallization, the thermal conductivity of the material, and the properties of the inner surface of the vessel containing the feed to be frozen. In this respect, it is also necessary to define the notions cooling/chilling rate and freezing rate as these two parameters are not identical, especially when the ambient temperature is not too low. The cooling/chilling rate can be controlled rather strictly, for instance, by using precision programmable cryostats, whereas the freezing rate corresponding to the rate of solvent crystallization depends on many factors, particularly on the supercooling depth. For instance, in the case of slow chilling of dust-free feed solutions containing dissolved polymeric precursors, the supercooling effect can be very pronounced [8, 41]. This effect then results in an initial high rate of crystallization, and at high crystallization rates the size of the forming solvent crystals is small. If there is no supercooling, then the lower the freezing temperature, the smaller the size of solvent crystals [42, 43] and, hence, the smaller the cross-section of macropores in the resulting cryogels (see [8, 22, 23, 29, 34, 44–46] and also Sect. 4.1 in [47] of this volume). However, supercooling leads to a deviation from the above-indicated regularity. One such example is given in Fig. 1, which shows the micrographs of chitosan cryogels prepared in frozen aqueous systems at −10, −15, and −30 °C [10]. The quantitative data obtained from the images, namely the number and weight averages of the pore diameters and the coefficient of polydispersity of the pores, are listed in Table 1. The results show that the average diameter of large pores in the cryogel formed at −10 °C is smaller than in cryogel prepared at −15 °C (compare Fig. 1a with b). The reason for such an effect is exactly the supercooling phenomenon.

In some cases, a spatial polymer network may form while the gelling system is in the supercooled state. Such a nonequilibrium state was reported both during chemical gelation processes like crosslinking polymerization as well as during chilling-induced noncovalent gelation. The primary ordinary gel thus formed in the supercooled state of the gelation system will be subjected to physical stresses upon the start of the freezing process due to the movement of the crystallization fronts. Such an effect has been registered upon very slow chilling (0.003 °C/min) of 100 g/L poly(vinyl alcohol) (PVA) aqueous solutions [48]. It was shown that a low-melting physical gel with a fusion temperature of ~21.5 °C forms before freezing of the system. In contrast, the equiconcentrated cryogels formed via conventional freezing, i.e., without a significant supercooling effect, had fusion temperatures of the order of 70–75 °C.

Several approaches have been proposed in order to exclude the influence of supercooling on the formation of different cryogels. These approaches include either special freezing profiles or the use of crystallization initiators. The former

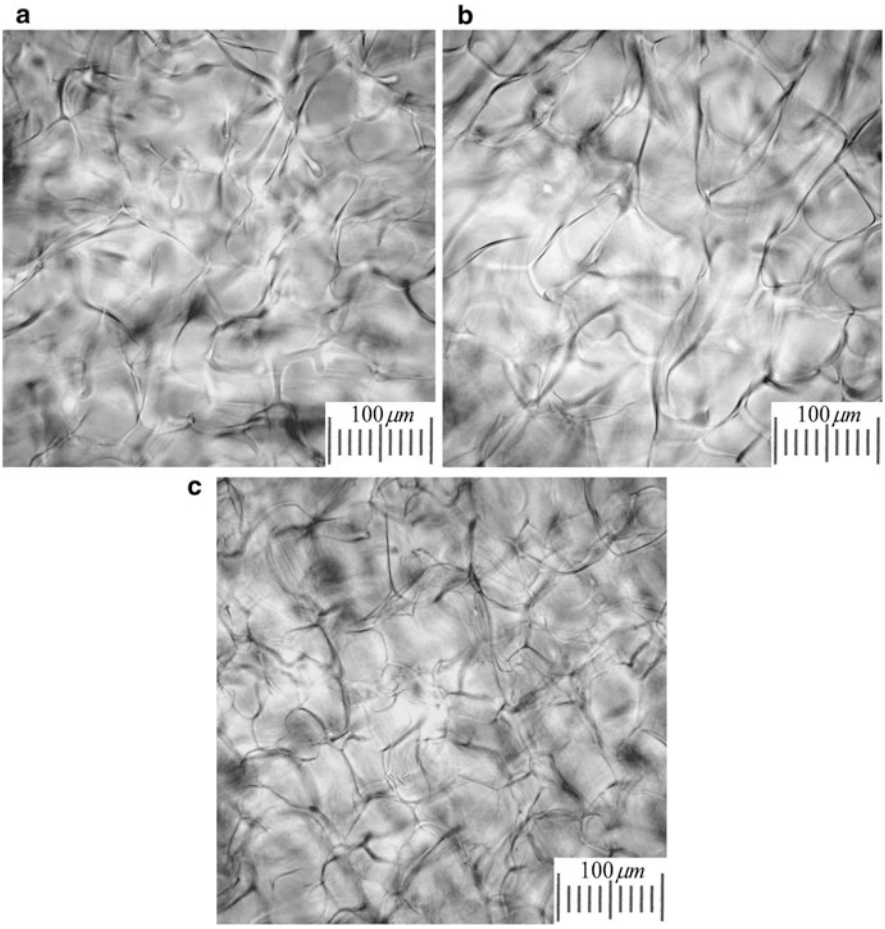


**Fig. 1** (**a**–**c**) Optical micrographs of 2-mm-thick disks of chitosan cryogels formed in moderately frozen aqueous solutions using glutaraldehyde as a crosslinker at −10 (**a**), −15 (**b**), and −30°C (**c**). (From [10] with permission from Springer)

**Table 1** Data on the quantitative analysis of microscopic images for the crosslinked chitosan cryogels formed at different negative temperatures

| Temperature of cryogel synthesis (°C) | $D_n$ (μm)[a] | $D_w$ (μm)[b] | $k$[c] |
|---|---|---|---|
| −10 | 57.4 | 70.1 | 1.22 |
| −15 | 72.3 | 87.0 | 1.20 |
| −30 | 44.3 | 56.0 | 1.26 |

From [10] with permission from Springer

[a]Number-average pore diameter: $D_n = (\sum(N_i \cdots D_i^3) : \sum N_i)^{1/3}$; the overall number of test objects in the micrograph is $\sum N_i$

[b]Weight-average pore diameter: $D_w = \{\sum(N_i \cdots D_i^6) : \sum (N_i \cdots D_i^3)\}^{1/3}$

[c]Coefficient of polydispersity: $k = D_w{:}D_n$

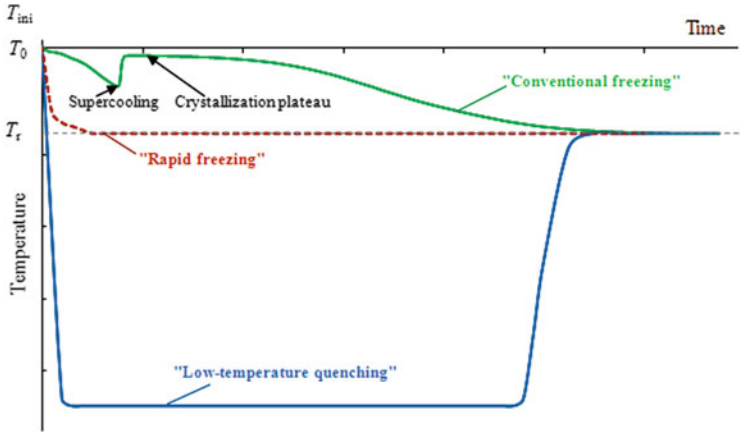


**Fig. 2** Freezing profiles of the reaction system according to the conventional, rapid, and low-temperature quenching procedures. $T_{ini}$ initial temperature of the system before the start of freezing; $T_0$ freezing point of the neat solvent; $T_r$ reaction temperature. (From [49] with permission from Springer)

variant can be subdivided into two techniques utilizing different freezing profiles, namely the rapid freezing and low-temperature quenching techniques. The character of these freezing profiles is shown schematically in Fig. 2. The rapid freezing procedure includes placing the feed system, immediately after commencing of the gel formation process, into a low-temperature bath (e.g., liquid nitrogen) for a short time, usually less than 1 min, to ensure fast solvent crystallization. This is followed by transfer of the feed into a cryostat for frozen storage at the desired subzero temperature $T_r$. The second procedure, namely low-temperature quenching, also uses liquid nitrogen for fast freezing of the system of interest, but for a longer time (0.5–1 h) in order to make the reaction system completely solid. Then, the feed is placed into a cryostat at a preset negative temperature $T_r$ (Fig. 2). Although both of these freezing procedures minimize the time period in the unfrozen state, they influence the dynamics of cryotropic gelation as well as the porous morphology of the resulting cryogels. In other words, the thermal prehistory of the feed during its freezing influences both the course of the cryotropic gelation and the gel properties. Such an influence was observed in the formation of poly(acrylamide) cryogels [23, 50] and in the linear cryopolymerization of acrylamide [49].

In this context, the use of "artificial" germs of crystallization looks rather attractive. For instance, crystals of silver iodide (AgI) are known to cause efficient ice formation in aqueous systems, thus preventing their supercooling [51, 52]. However, because of the polyvalent nature of both Ag and I atoms, this salt can act as a scavenger for free radicals and ion-radicals. Therefore, introduction of AgI powder into the solution of monomers will affect the course of cryogel formation via the radical reactions. This necessitates certain preliminary tests in order to make sure that such an additive has no undesired influence on cryotropic gelation. In this regard, ultrasound treatment of the initial feed as it is cooled below the freezing

point can be a better way to suppress supercooling. Such a physical impact on the liquid system causes cavitation of gas microbubbles within the whole volume of the sample, thus resulting in uniform nucleation of the solvent crystallization [53]. However, no practical examples of implementing this approach for the preparation of polymeric cryogels are known so far to the authors of this review. This is probably due to the absence of laboratory-scale ultrasound equipment suitable for cryotropic gelation procedures.

## *2.3 Incubation of the Gelation System in a Frozen State*

Keeping the gelation system in a frozen state at a moderate negative temperature is the main stage in the synthesis of covalent cryogels, since the chemical reactions leading to gelation mainly occur during this time period [8]. In the case of physical cryogels, the pattern is not so straightforward and will be discussed later. Nonetheless, in both cases, polymeric cryogels form within the volume of the unfrozen liquid microphase (UFLMP, also called the "nonfrozen liquid microphase") where the precursors are concentrated as the solvent starts to crystallize [8]. Therefore, the concept of UFLMP will be discussed in more detail.

The term "unfrozen liquid microphase" was proposed by Sergeev and co-authors in 1973 for designating the liquid fraction at a particular negative temperature in a macroscopically frozen system [54]. This concept was developed in the course of exploration of various chemical reactions occurring in the non-deeply frozen multicomponent solutions of low molecular weight reactants. These studies, beginning from the initially empiric observations [55–61], then generalized by Pincock [62], and leading to a rather harmonious kinetic theory elaborated by Sergeev and Batyuk with coworkers [54, 63, 64], revealed the following three fundamental features of such processes and their mechanisms:

1. When the initial molecular or colloidal solution is non-deeply frozen, although the system looks like a completely solid matter, it is heterophase at a microscopic level and contains, along with the solvent polycrystals, a certain unfrozen fraction, UFLMP. Thus, the moderately or non-deeply frozen systems are those where UFLMP is still present. The existence of UFLMP at temperatures both above and below the eutectic point of the particular system is confirmed by different physicochemical methods, e.g., by the narrow NMR signals of the solutes [8, 41, 50, 52, 63–72] and by the shape of ESR spectra characteristic of the liquid microenvironment of spin probes [8, 63, 73–76]. The temperature boundary of the existence of UFLMP is stipulated by several factors such as the nature of the solvent, the amount of solutes, their physicochemical properties (e.g., molecular weight [77]), the flexibility of the chains in the case of polymeric precursors, thermal prehistory of the system during its freezing if the phase equilibrium is not yet attained, etc.

2. The concentration of solutes or dispersed colloid-size particles is increased because of their expulsion into the volume of UFLMP as the solvent is crystallized. This cryo-concentration effect is one of the major factors responsible for the increase in the rate of the chemical reactions and intensification of intermolecular interactions inside the unfrozen inclusions, which act as microreactors. Provided the reactants are easily soluble compounds and are completely concentrated within the UFLMP, the concentrating extent $\beta$ at a certain negative temperature $T$ can be estimated using the following formula [54]:

$$\beta = \frac{T_0 - T}{\Delta \sum C_i} \tag{1}$$

where $T_0$ is the crystallization point of the solvent, $\Delta$ is its cryoscopic constant, and $C_\mathrm{i}$ is the initial concentration of the solute $i$. Note that the concentrating extent $\beta$ is the ratio of the total concentration of solutes within the UFLMP to that in the initial solution. It is also possible to measure the $\beta$ values experimentally from the NMR spectra of such frozen systems, provided that their compositions are not too complex and the solvent is suitable for use in the NMR technique.

3. Owing to the competition of several oppositely directed factors, the temperature dependence of the efficiency of the process in terms of the reaction rate or the yield of the final products is, as a rule, bell-shaped. According to the structure–kinetic model developed by Sergeev-Batyuk [63, 64], the temperature of the maximum reaction rate ($T_{\mathrm{max,r}}$) of cryochemical reactions between low molecular weight substances with an order higher than 1 is given by the following equation:

$$T_{\mathrm{max},r} = \left( \frac{E^2}{4R^2 \left[ \left( \sum_j n_j \right) - 1 \right]^2} + \frac{ET_0}{R \left[ \left( \sum_j n_j \right) - 1 \right]} \right)^{0.5} - \frac{E}{2 \left[ \left( \sum_j n_j \right) - 1 \right]} \tag{2}$$

where $E$ is the activation energy of the reaction, $R$ is the universal gas constant, and $n_j$ is the reaction order with respect to the $j$th component.

Most of these features of cryochemical reactions are also of great significance for cryotropic gelation processes [8]. Moreover, if the system contains polymeric solutes, the still-liquid fraction can exist even at rather low temperatures and such

systems are very sensitive to the thermal prehistory, i.e., the temperature profile used to reach the preset temperature point. For instance, upon freezing of concentrated aqueous PVA solutions, the presence of mobile water molecules was detected by NMR even at –50 °C [78]. In addition, since the relaxation processes in viscous liquids are very slow, the characteristics of UFLMP (such as its volume during freezing and defrosting stages) differ significantly, leading to hysteresis phenomena [76, 79]. Similarly to cryochemical reactions, the gelation rate and the gel-fraction yield of cryotropic gelation processes, as well as the mechanical characteristics of the final cryogels, are strongly dependent on the frozen storage temperature and are also bell-shaped. Such a character of temperature dependences was observed during the formation of covalent cryogels from monomeric [7, 8, 22, 23, 80–85] and macromolecular precursors [7, 8, 10, 27–29, 32, 45, 46, 86–88], for some physical cryogels [7, 8, 34, 44, 48, 89–103] as well as during linear cryopolymerization processes [49, 72, 104–106].

Based on the concept of UFLMP, the scheme of cryotropic gelation processes can be depicted by the simple diagram in Fig. 3, which reflects all the essential features of the systems [107]. When the initial feed containing the monomeric or polymeric precursors freezes at a moderate negative temperature (Fig. 3a), the frozen system consists of at least two phases, namely the solvent polycrystals and the UFLMP where the solutes are concentrated (Fig. 3b). Due to the considerable increase in the concentration of solutes in these liquid-like inclusions, the gelation can intensify and result in the formation of a 3D polymeric network within the volume of this phase. Thus, a cryogel is formed in a solution of the precursors that is much more concentrated than the initial solution. After thawing of the frozen system, numerous macropores arise in place of the melted solvent crystals (Fig. 3c). Hence, the crystals act as a pore template or porogen, whereas the structure of gel phase (the pore walls) is determined by the initial concentration of gelling agents and by the number of crosslinks of the respective spatial networks.

## *2.4 Thawing of the Frozen System*

Thawing of the gelation system after incubation in a frozen state for a necessary time period is the last basic stage of the cryotropic gelation processes. The least energy-consuming procedure is a simple spontaneous thawing of the frozen system at an appropriate positive temperature. The conditions of thawing are generally unimportant as long as the formation of a particular covalent cryogel is mainly completed before this stage, i.e., if the reactions are virtually stopped and the gel-fraction yield reaches the maximum possible value. However, it is sometimes necessary to stop the gelation prior to its completion, e.g., for studying the variation in gel-fraction yield with reaction time [7, 8, 22, 23, 27, 28, 32, 86]. In this case, fast defrosting techniques should be employed in order to thaw the reacting system as quickly as possible, but without overheating. The reactions may also be stopped either by intense dilution or by addition of a relevant chemical inhibitor, e.g., free

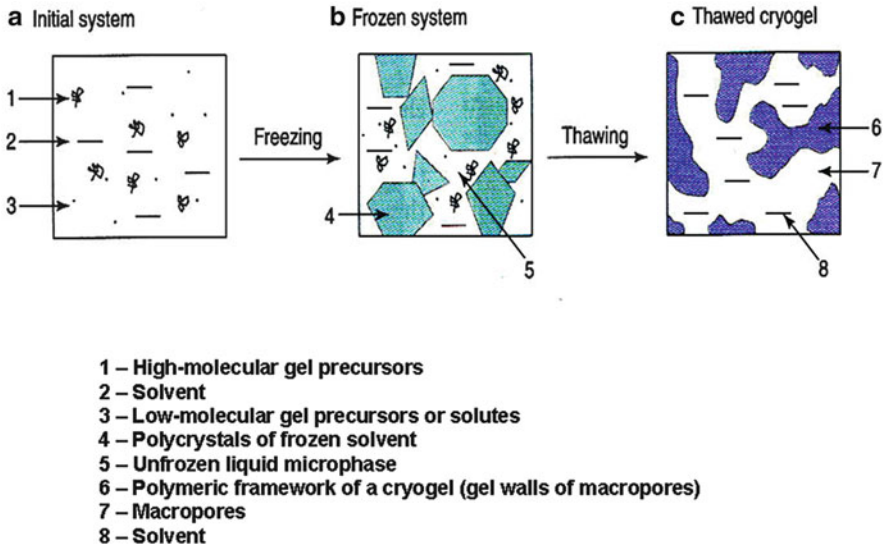


**Fig. 3** (**a**–**c**) Conceptual diagram of the formation of polymeric cryogels. (From [107] with permission from Elsevier)

radical scavengers in radical-type reactions. Sometimes, a short-term microwave exposure can be used for fast defrosting [10, 65], or rapid heating of the frozen system with a programmed rate.

Similarly to the non-equivalence of the chilling and freezing rates of the initial feed, the rates of heating and defrosting (i.e., melting of the solvent crystals) should also be distinguished. Whereas the heating rate is easy to govern using programmable cryostats, the defrosting rate corresponding to the melting of solvent crystals is subject to multiple factors and is difficult to control.

The conditions of the thawing stage are often much more important in the preparation of physical cryogels than for covalent gels. If the physical cryogels are formed rapidly upon freezing of the feed containing certain precursors such as starch polysaccharides [14, 15, 98, 108, 109] or agarose [33, 34], the contribution of the thawing conditions to the final result is not very substantial. However, for slow gelation systems like the solutions of PVA [7, 8, 44, 48, 93–95, 97, 99, 110–114] or locust bean gum [100, 102, 115], the thawing conditions become significant. The plots in Fig. 4 illustrate the influence of the thawing rate on the shear modulus and the fusion temperature of physical PVA cryogels [44]. The cryogels were prepared by freezing of PVA solutions at −20 °C for 18 h followed by thawing at different rates. The different curves in Fig. 4 correspond to initial PVA concentrations of 120, 100, and 80 g/L. Both the shear modulus and the fusion temperature of the cryogels gradually increase as the thawing rate is decreased. For instance, at a PVA concentration of 80 g/L (curve 3), decreasing the thawing rate from 0.3 to 0.003 °C/min increases the modulus, i.e., the rigidity of the cryogels from 2 to 13 kPa. This effect is even more pronounced in more concentrated samples. Thus, for the system

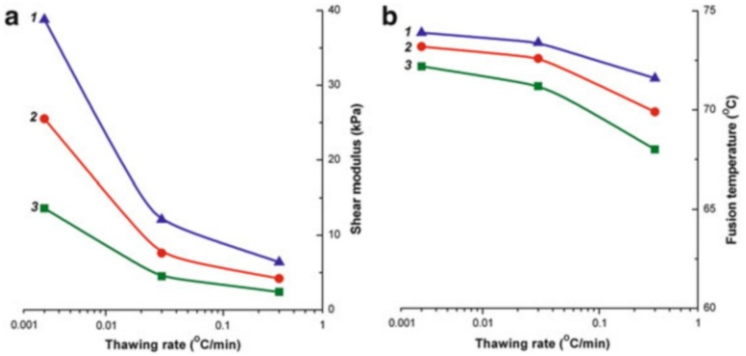


**Fig. 4** Effect of the thawing rate on (**a**) the shear modulus and (**b**) the fusion temperature of PVA cryogels prepared by freezing of aqueous polymer solutions at −20 °C for 18 h. PVA concentrations were 120 (*1*), 100 (*2*), and 80 g/L (*3*). (Plotted based on data from [44])

containing 120 g/L PVA (curve 1), the modulus increases by factors of 1.77 and 5.64 as the heating rate is increased from 0.3 to 0.03 and 0.003 °C/min, respectively. The slow-thawed samples are also more thermoresistant, as evidenced from the fusion temperatures (Fig. 4b), and the enthalpy of their fusion is also considerably greater than that of fast-thawed samples. Note that when the moderately frozen PVA solutions were heated with a high rate such as 15 °C/min, no cryogels were obtained at all. Thawing of the samples at such a high rate led to the formation of viscous and turbid (heterogeneous) fluid instead of a rubber-elastic gel [44, 93, 95], whereas the efficiency of PVA cryotropic gelation (such as the yield of gel-fraction) increases when defrosting is slowed down [113]. The results thus show that the slower the thawing rate, the larger the modulus (i.e., strength of the resulting cryogels) and the heat endurance. The reason is the fact that, since gel formation proceeds slowly in highly viscous UFLMP medium, the sol–gel transition in such systems requires a long time to occur so the PVA microcrystallites in the nodes of spatial network become more perfect at slow thawing rates.

Studies on the fine details of the processes taking place at the thawing stage have shown that the formation of a supramolecular 3D physical network of PVA cryogels proceeds most intensively within the subzero temperature range between 4 and 1 °C below the melting point of the system [44, 93, 99]. In NMR experiments, the well-resolved $^{13}C$ NMR signals of frozen samples in this temperature range indicate segmental mobility in PVA chains [78], which is a necessary factor for effective interchain interactions. Hence, the longer the system stays within this temperature range during defrosting, the higher is the gel formation efficiency. For instance, at a heating rate of 3 °C/min, the temperature increases from –4 to –1 °C within 1 min, while at a rate of 0.003 °C/min, it takes about 17 h [111]. Thus, slow-enough defrosting ensures a prolonged passage time across the temperature diapason, which favors the formation of stronger PVA cryogels. At low heating rates, the system has sufficient time for slow PVA microcrystallization, which promotes the extent of intermolecular contacts. This leads to an increased degree of hydrogen-

binding cooperativity rather than to an increase in the number of microcrystallites. The former is manifested in a substantial increase in the fusion enthalpy, whereas the latter leads to a moderate increase in the fusion temperature of cryogels, i.e., to a small change in the entropy factor. At a qualitative level, there is an analogy with the crystallization of low molecular weight substances upon cooling of their hot saturated solutions; when the system is cooled slower, less crystals are formed, but their sizes are larger and the crystalline lattice becomes more perfect [116].

The regime of the thawing stage also influences markedly the macroporous structure of such noncovalent cryogels. During sufficiently slow heating of frozen samples, the gel formation occurs at subzero temperatures and, simultaneously, the re-crystallization of the frozen solvent is intensified, which has an impact on the porous morphology of the resulting cryogels. This influence is demonstrated by the micrographs in Fig. 5, which show thin sections of PVA cryogels formed at different heating rates. The cryogels were prepared from aqueous PVA solutions frozen under identical thermal conditions but defrosted at heating rates of 0.3 (Fig. 5a), 0.03 (Fig. 5b), and 0.003 °C/min (Fig. 5c). Because slowing of defrosting of the frozen system results in an increase in the rigidity of the corresponding cryogels (Fig. 4a), it can be suggested that such changes in their mechanical parameters are caused not only by the strengthening of the gel phase of heterogeneous material, but also by a decrease in the inhomogeneity of its structure, where the macropores act as defects. This was indeed observed. As seen in Fig. 5, the slower the thawing of the frozen system, the less pronounced is the orientation of the texture elements. Most likely, this effect is associated with the re-crystallization of ice at slow heating of the frozen samples when the system has enough time to balance the temperature fields, and the processes of mass transfer participating in re-crystallization become equiprobable in all directions. In this regard, the texture of the sample shown in Fig. 5b seems to be transient between the clearly unidirectional texture of the rapidly thawed sample (Fig. 5a) and the texture of a very slowly defrosted sample pierced with intersecting pores (Fig. 5c). In addition, slowing down of the heating rate at the thawing stage leads to a decrease in the total porosity of PVA cryogels and in a slight diminution in the average cross-section of the macropores (see caption to Fig. 5).

Another freeze–thaw procedure having a strong impact on the properties and porous morphology of noncovalent cryogels such as PVA-based cryogels is the use of multiple or iterative “freezing–frozen storage–defrosting” cycles. This variant of cryogenic treatment results in the growth of the crystallinity degree of PVA cryogels [117–120]. Such thermal cycling is able to increase considerably the strength of physical cryogels and their heat endurance [111, 121–133]. One of the reasons for this effect is the fact that the gelation system passes across the above-indicated subzero temperature zone several times, which is very favorable for such cryotropic gel formation. Thus, the durations of the several traversals at the subzero temperature range are virtually summed. Such a “temperature saw” also affects the pore morphology of the resulting cryogels. This is illustrated by the micrographs in Fig. 6, which show the effect of the number of cycles on the pore morphology of PVA cryogels. The second freeze–thaw cycle results in a significant increase both

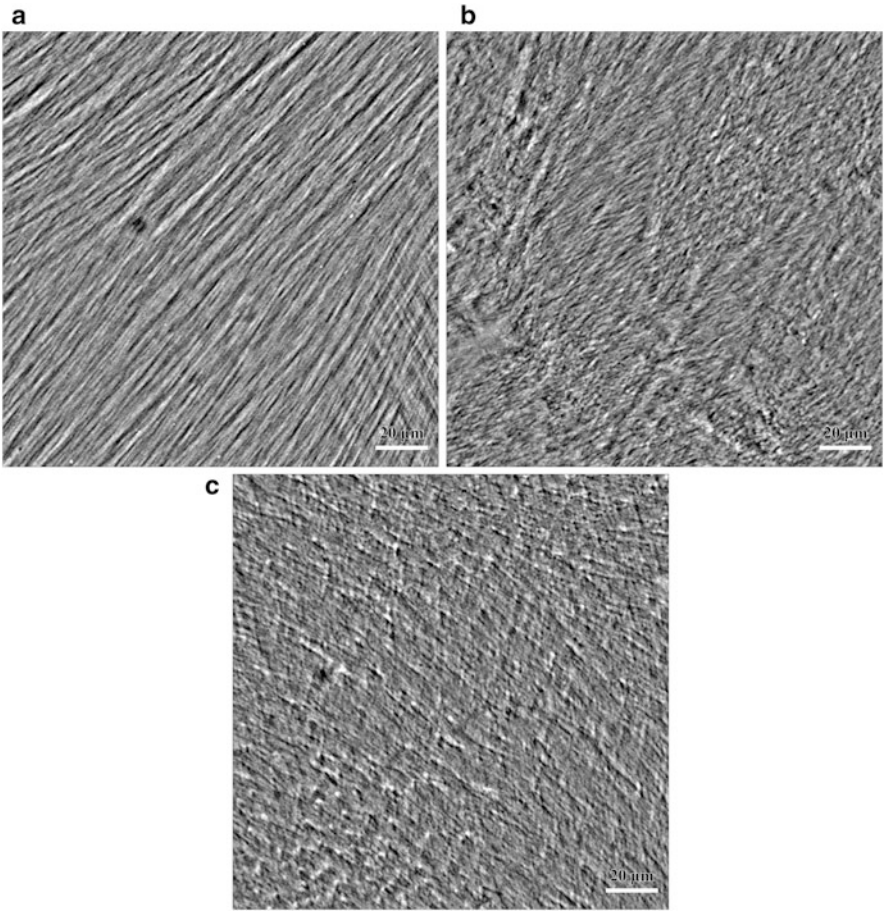


**Fig. 5** (**a**–**c**) Optical micrographs of thin sections of PVA cryogels prepared by freezing of aqueous polymer solutions (100 g/L) at −20 °C for 18 h and then thawed at a rate of 0.3 (**a**), 0.03 (**b**), and 0.003 °C/min (**c**). The average size of macropores was 2.8 (**a**), 2.7 (**b**), and 2.5 μm (**c**). The fraction of macropores was 61.3 (**a**), 53.1 (**b**), and 49.6 % (**c**). *Scale bars*: 20 μm. (From [44] with permission from Springer)

in the average size of macropores (by a factor of 2–3) and in the total (macro) porosity (by ~30 %), whereas the subsequent cycles cause only a slight increase in these characteristics. At the same time, both the rigidity and the fusion temperature of the cryogels continue to increase with every following cycle. These experimental results demonstrate that the pore space of PVA cryogels is mainly expanded during the second freezing step when the ice crystals grow inside the micrometer-sized pores formed after the first freeze–thaw cycle, whereas the gel formation processes in the gel phase continue to occur at every subsequent thawing stage.

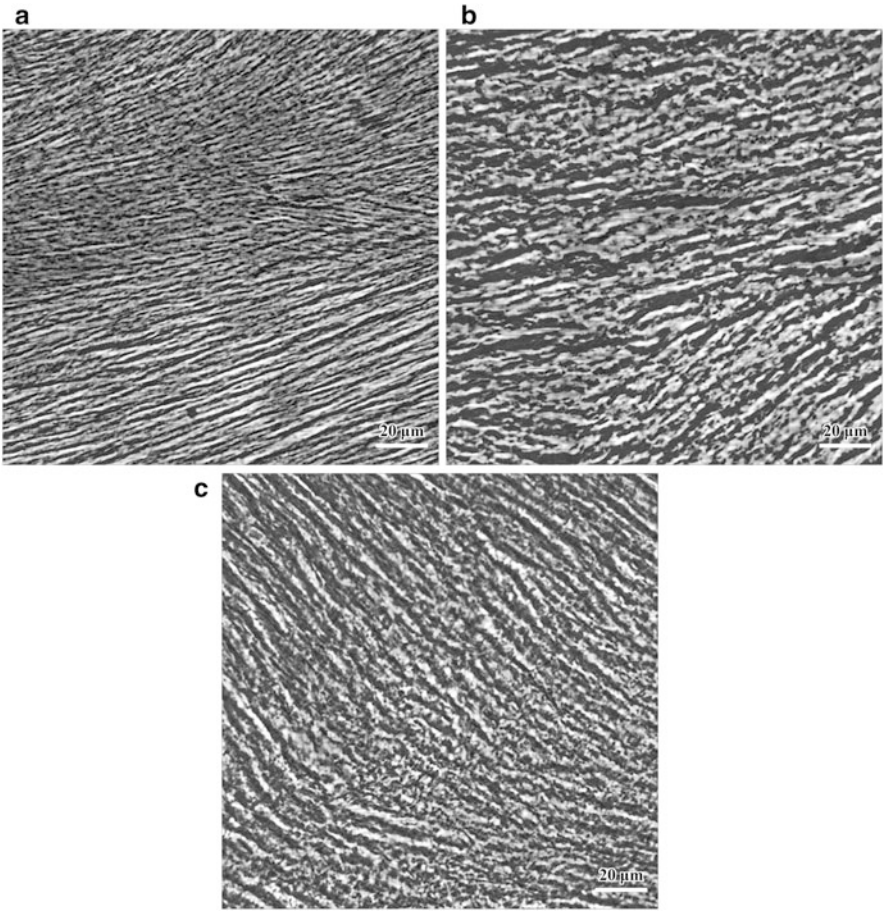


**Fig. 6** (**a**–**c**) Optical micrographs of thin sections of PVA cryogels prepared by iterative freezing of aqueous polymer solutions (100 g/L) at −20 °C for 18 h and then thawed at a rate of 0.3 °C/min. The number of freeze–thaw cycles was 1 (**a**), 2 (**b**), and 5 (**c**). The average size of macropores was 2.8 (**a**), 6.1 (**b**), and 6.5 μm (**c**). The fraction of macropores was 61.3 (**a**), 80.8 (**b**), and 79.8 % (**c**). *Scale bars*: 20 μm. (From [129] with permission from Springer)

In summary, we can conclude that the conditions of each step in the preparation of cryogels affect the course of gelation and, hence, the properties and structure of the resulting gel materials. The extent of the influence of the processing conditions is different and depends on the chemical nature of the cryogel precursors, their initial concentrations, and on the temperature regimes of the cryogenic stages, i.e., on the parameters of freezing, frozen storage, and defrosting. Therefore, there is no general procedure for the preparation of any cryogel; for each specific case a preliminary search for the most suitable conditions is required to obtain the materials with desired characteristics. Such a search can sometimes involve a lot of effort; however, it gives useful information regarding the factors that are important for each kind of cryotropic gelation process as well as the fine details of the corresponding mechanisms.

# 3 Specific Effects of Gel Formation in Moderately Frozen Systems

## *3.1 Apparent Decrease in the Critical Concentration of Gelation*

One of the principal conditions for conventional gelation at positive temperatures is that the concentration of the precursors in the feed has to exceed a certain boundary value, called the critical concentration of gelation (CCG) [2]. The same is also true for cryotropic gel formation. In the early systematic studies on the main factors influencing the properties of freeze–thaw gels, it was found that cryogels can be obtained at initial precursor concentrations considerably lower than the critical values needed for gel formation at positive temperatures. Such a decrease in CCG is inherent in the formation of both chemically crosslinked cryogels [19, 20, 26, 27] and noncovalent gels [12]. This effect has been observed for cryostructuring in moderately frozen aqueous systems [20, 26, 27] as well as in organic systems [27]. Figures 7 and 8 represent typical examples of such an effect. These data concern covalent-type gelation in "solvent–polymeric precursor–crosslinking-agent" systems, namely crosslinked chitosan gels in an aqueous medium (Fig. 7) and crosslinked poly(styrene) gels in nitrobenzene medium (Fig. 8). Figure 7a shows the scheme of the crosslinking reaction of chitosan using glutaraldehyde as a crosslinker. In Fig. 7b, c, the gel-fraction yield is plotted against the initial chitosan concentration and the initial molar ratio of aldehyde to amine groups, respectively. The two curves represent data for chitosan gels formed at −8 and 24 °C. It is seen that the crosslinking of chitosan with glutaraldehyde at −8 °C results in the formation of cryogels at about one third of the initial polymer concentration compared with the formation of conventional gels at 24 °C. Moreover, there is also an approximately threefold difference in the critical crosslinking agent concentration in terms of the molar ratio of aldehyde to amine groups (Fig. 7c). The reason for this phenomenon is the cryo-concentration effect (Fig. 3), since the gel phase of cryogels forms within the UFLMP, which is more concentrated than the initial solution. Therefore, the decrease in CCG in cryotropic gel formation is an apparent decrease due to the confinement of the reacting species to the microreactor UFLMP [8]. Qualitatively, the same trend was observed during the synthesis of covalent cryogels in organic media, which is exemplified by the crosslinking of poly(styrene) using 4,4′-xylylene-dichloride via the Friedel–Crafts reaction (Fig. 8a). Such cryogels possess a wide-pore spongy texture and can be obtained in moderately frozen nitrobenzene ($T_0$ = +5.5 °C). In Fig. 8b, the gel-fraction yield is plotted against the polymer concentration for gels prepared at relative temperatures $\Delta T$ of −19 °C and +28 °C. The critical polymer concentration at $\Delta T$ = −19 °C is six times lower than that at 28 °C. Thus, the data in Figs. 7 and 8 demonstrate the universal character of the effect under discussion in both aqueous and organic media.

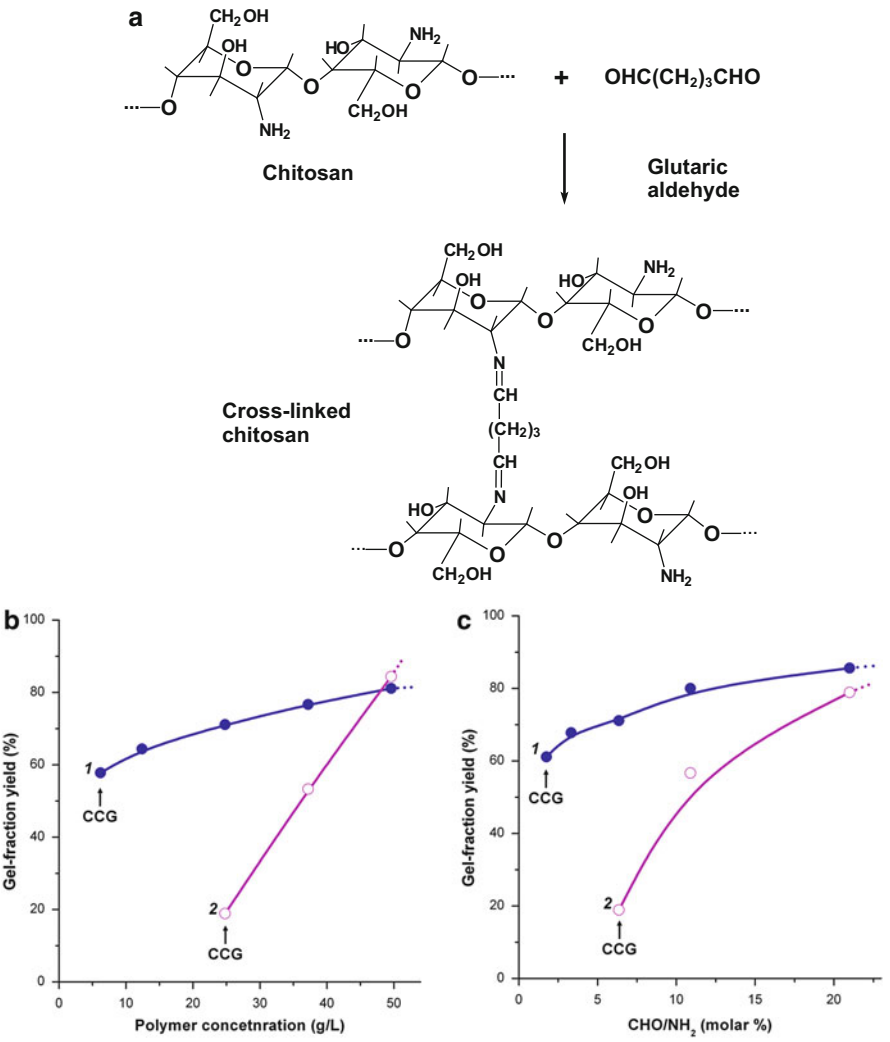


**Fig. 7** (**a**) Crosslinking reaction of chitosan using glutaraldehyde as a crosslinker in aqueous acetic acid solutions. (**b**, **c**) Gel-fraction yield plotted against the initial chitosan concentration (**b**) and the initial molar ratio of aldehyde to amine groups (**c**). Gelation temperature was −8°C (*curve 1*) and 24 °(*curve 2*). *CCG* critical concentration of gelation (Plotted based on the data from [26])

Another interesting example illustrating the cryo-concentration effect is the shift of pH during the acetalation reactions between the OH groups of poly(vinylalcohol-*co*-vinylacetate) (80:20 by mole) and CHO groups of glutaraldehyde (Fig. 9a). The mechanism of this reaction in acidic media includes the initial protonation of the carbonyl of aldehyde [134]. Thus, at low concentrations of hydroxonium ions, the reaction rate is slow and, therefore, the gels are usually synthesized at pH $\leq$ 1.5–1 in order to ensure high-enough yield of the gel-fraction [135, 136]. In Fig. 9b, c, the

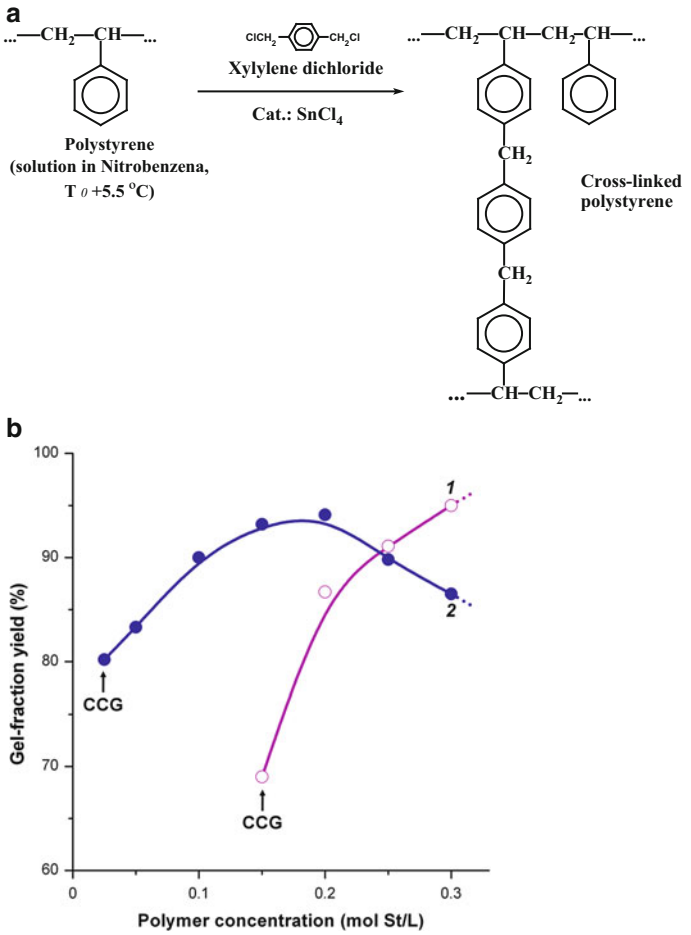


**Fig. 8** (**a**) Crosslinking reaction of polystyrene using xylylene dichloride as a crosslinker in nitrobenzene. (**b**) Gel-fraction yield plotted against the initial polymer concentration expressed in molarity of styrene (*St*) units. Relative temperature ($\Delta T$) was −19 °C (*curve 2*) and 28°C (*curve 1*). (Plotted based on the data from [26])

gel-fraction yield is plotted against the initial pH of the polymer solution for gelation at 24 °C and for cryogelation at −12 °C, respectively. The boundary pH value of the feed at which cryogels can be generated (Fig. 9c) has shifted by about 0.5 units toward less the acidic zone as compared to the case of conventional gels (Fig. 9b). Such a difference in pH corresponds to about a threefold difference in the concentration of $H^+$ ions. Thus, the apparent decrease in CCG due to the cryo-concentrating effect is reflected in this example with an increase in medium acidity rather than in the gel precursor concentration [7]. It is also interesting to compare the osmotic characteristics, e.g., the equilibrium swelling capacities of such gels and cryogels. Figure 9d, e shows the equilibrium swelling degrees of the gels and

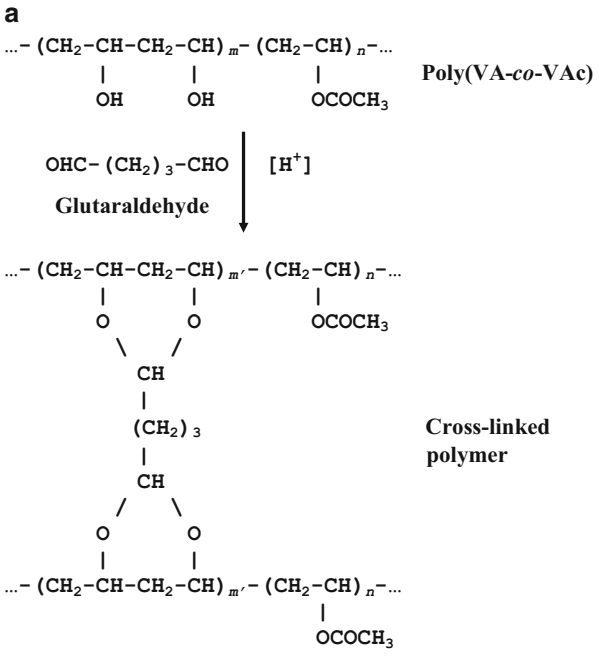


**Fig. 9** (continued)

cryogels in water, plotted against the pH of the initial feed solution. The homophase chemically crosslinked PVA gels swell strongly in water (Fig. 9d), and their swelling degree increases considerably (from tens of grams to more than 100 g water per gram of dry polymer) as the pH of the feed rises from 1 to 3 due to the decreasing crosslinking efficiency. However, the heterophase sponge-like cryogels are not only formed under apparently less acidic initial conditions, but also their gel phase swells significantly less than the corresponding homophase gels (from several to 20–30 g water per gram of dry polymer). This indicates a higher crosslinking extent of the 3D networks in the cryogel samples as compared to the conventional gels synthesized under identical crosslinking agent content and pH. The reason for the different swelling behavior of PVA gels and cryogels is because the cryo-concentration processes in UFLMP give rise to an increase in the concentrations of both the gel precursors and $H^+$ ions. This facilitates the formation of a more concentrated, highly crosslinked gel matrix forming the pore walls in such cryogels.

In this connection, we should note that for such wide-pore gel matrices, the swelling capacity of the gel phase is an essential indicator of the polymer content in this phase and of the crosslinking extent. By contrast, the total volume occupied by such swollen gel materials is a less informative indicator for the properties of the polymeric network. This is due to the fact that the volume occupied by free solvent inside the capillary-sized pores accounts for the greater part of the liquid absorbed by these wide-pore sponges. In turn, the fraction of tightly bound solvate liquid

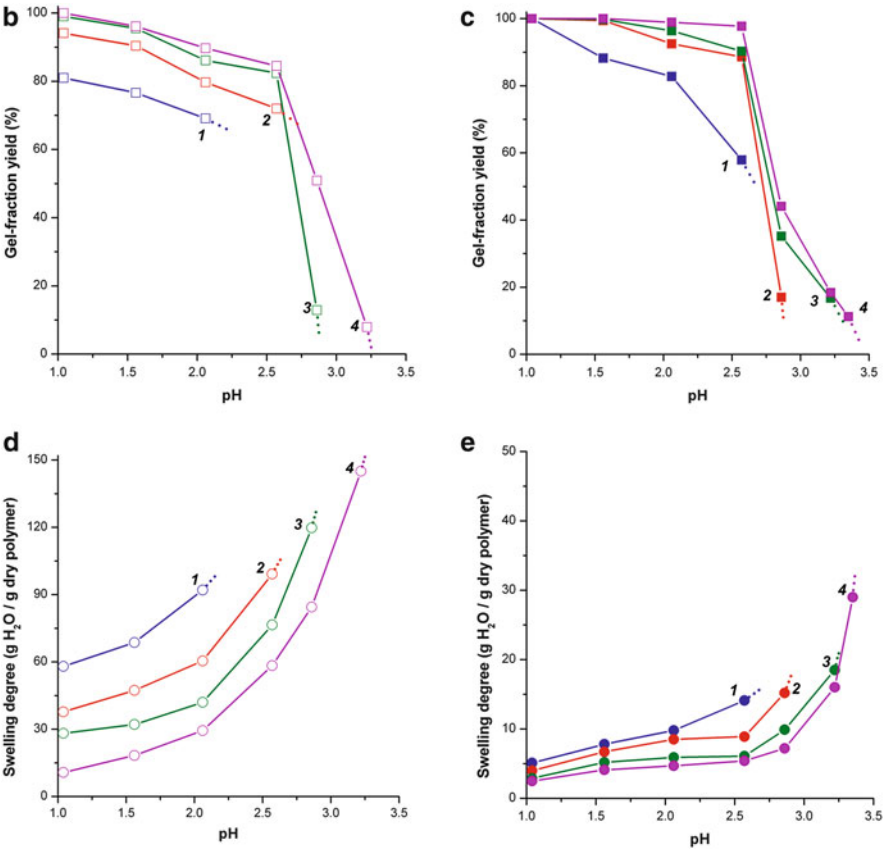


**Fig. 9** (**a**) Crosslinking reaction of poly(VA-*co*-VAc) (80:20 by mole) using glutaraldehyde as a crosslinker in aqueous acid solution. (**b**–**e**) The gel-fraction yield (**b**, **c**) and the swelling degree of the gels in water (**d**, **e**) plotted against the initial pH of the feed solution. Gelation temperature was 24 °C (**b**, **d**) and −12 °C (**c**, **e**). Polymer concentration was 50 g/L. Glutaraldehyde molar ratio with respect to OH groups in the polymer was 5.6 (*curve 1*), 11.2 (*curve 2*), 16.8 (*curve 3*), and 22.4 mol % (*curve 4*). (Plotted based on the data from [8])

inside the pore walls is only a small share of the whole volume of liquid soaked up by such polymer materials. The net amount of the free liquid is determined by the inner volume of the large pores, which depends on the total mass of solvent crystals formed in the system during the cryotropic gelation process and, to a certain extent, on the size of these crystals. The liquid from the capillaries of the sponge-like cryogels can be squeezed off by mechanical compression, sometimes almost completely [46], whereas the solvate fraction can only be removed from the polymer matrix by intense drying, i.e., by heating under reduced pressure. Thus, the total volumetric swelling degree does not characterize the osmotic properties of the gel pore walls in the wide-pore cryogels. However, in some cases, comparison

of the swelling behavior of cryogel matrices in different solvents can be an indicator of the affinity of the capillary system of cryogels with respect to the tested liquids.

The apparent decrease in CCG is also characteristic during the formation of polymerization-type cryogels. This phenomenon was first observed upon comparison of the critical concentrations of vinyl and divinyl comonomers, namely acrylamide and *N*,*N*′-methylene(bis)acrylamide, for the formation of poly(acrylamide) gels and cryogels [7, 8, 19–23]. At room temperature, the CCG for this gelation system lies in the vicinity of 2 wt% and also varies depending on the ratio of vinyl and divinyl components [137–139]. However, when the polymerization occurs in a moderately frozen medium, wide-pore sponge-like poly(acrylamide) cryogels can be prepared using at least half the concentration of the comonomers [7, 19]. The physicochemical features of such gelation systems are considered in more detail in [47]. Here, it is reasonable to emphasize only that the effect of an apparent decrease in CCG is common for the formation of any type of chemically crosslinked cryogels, and this effect is mainly determined by the increase of precursor concentration in the volume of UFLMP as the solvent freezes out.

The question is whether the same decrease in CCG is also inherent in the formation of physical cryogels. The answer in most cases is obviously, yes. For instance, the gelation process of aqueous solutions of locust bean gum was investigated both at positive and negative temperatures. Locust bean gum is a polygalactomannan gum consisting of poly(1,4-β-D-mannose) main chain and 1,6-α-D-galactose pendant chains with a mannose to galactose ratio of 1:4 [140]. Solutions (1–4 wt%) of locust bean gum remain fluid during prolonged storage at positive temperatures and they transform into very weak gels only after 2–3 months [141]. However, cryogenic treatment of the same feed systems produces cryogels within a short period of time [100, 102, 115, 142–144]. Thus, the effect of CCG decrease was clearly demonstrated for such cryogels. They are thermoreversible, i.e., the cryogels can be melted by heating and they form again after a new freeze–thaw cycle. The morphology of the cryogels based on locust bean gum is heterogeneous; they resemble soft sponges as long as the initial polysaccharide concentration is lower than 2.0–2.5 wt%. Such sponge-like cryogels exclude free liquid under a slight compression. Although cryogenic treatment of more concentrated locust bean gum solutions also yields gel materials, they do not exclude free liquid under a moderate pressing. However, the latter gels are similar to the physical PVA cryogels in that they are also macroporous because, during cryotropic gel formation, ice polycrystals act as porogens and macropores of various sizes and architecture remain in the cryogel body after thawing.

There are also other examples of the manifestation of a CCG decrease during the formation of noncovalent cryogels. The precursors (i.e., polysaccharides, proteins, synthetic polymers) together with the conditions of gel formation processes and the appearance of the final material are listed in Table 2. These data demonstrate the universal character of the CCG decrease in both aqueous and organic media during cryotropic gelation as compared to conventional gelation. The best studied among the processes of the formation of noncovalent cryogels is the cryotropic gelation of PVA solutions. The reason for this is twofold: First, the final “products”, i.e., the

**Table 2** Influence of the freeze–thaw treatment on the solutions of polymeric precursors capable of forming physically crosslinked gels

| Precursor | Precursor concentration in the feed (wt%) | Solvent | Temperature of the gelation process (°C) | Appearance of the samples after the gel formation process | References |
|---|---|---|---|---|---|
| Agar-agar | 0.5 | Water | +20 | Rather weak gel | [12] |
| | | | −10 | Sponge-like cryogel | |
| | 1.0 | | +20 | Weak gel | |
| | | | −10 | Sponge-like cryogel | |
| Agarose (low-gelling-temperature brand) | 0.5 | Water | +20 | Jelly-like system | [7] |
| | | | −20 | Weak sponge-like cryogel | |
| Amylopectin | 1.0 | Water | +18 | Thin precipitate | [98] |
| | | | −18 | Non-spongy cryogel | |
| | 5.0 | | +18 | Very viscous paste | |
| | | | −18 | Non-spongy rigid cryogel | |
| Gelatin (A-type) | 0.5 | Water | +20 | Liquid | [12] |
| | | | −10 | Sponge-like cryogel | |
| | 1.0 | | +20 | Liquid | |
| | | | −10 | Sponge-like cryogel | |
| | 1.5 | | +20 | Very weak gel | |
| | | | −10 | Sponge-like cryogel | |
| Locust-bean gum | 0.3 | Water | +18 | Turbid liquid | [100, 115] |
| | | | −30 | Spongy cryogel | |
| | 3.0 | | +18 | Viscous opaque paste | |
| | | | −30 | Non-spongy cryogel | |
| Maltodextrin[a] | 12.5 | Water | +18 | Opalescent liquid | [101] |
| | | | −24 | Spongy weak cryogel | |
| Oat β-glucan | 3.0 | Water | +22 | No gel formation | [145, 146] |
| | | | −18 | Spongy cryogel | |
| Potato starch | 2.5 | Water | +18 | Rather weak starch gel | [147] |
| | | | −18 | Sponge-like cryogel | |
| PVA[b] | 15.0 | Water | +25 | Mechanically weak gel | [13] |
| PVA[c] | 10.0 | Water | +20 | Liquid | [12, 92] |
| | | | −10 | Non-spongy cryogel | |
| | | | −20 | Rather rigid cryogel | |
| | 16.0 | | +20 | Liquid | |
| | | | +2 | Very weak gel | |
| | | | −10 | Rigid cryogel | |
| | | | −20 | Rigid cryogel | |
| | 13.0 | DMSO | $\Delta T = +1.6$ | Liquid | [12] |
| | | | $\Delta T = -28.4$ | Rather rigid cryogel | |

[a]Molecular weight 8 kDa
[b]Duration of the incubation at gelation temperature 12 days
[c]Molecular weight 69 kDa

noncovalent PVA cryogels, possess outstanding mechanical and thermophysical properties. Second, owing to the very simple structure of the polymer itself, they are very convenient model systems for studying the fine mechanisms of cryotropic noncovalent gelation [8, 111, 112, 127, 129, 130, 148–152]. The shift in CCG upon the formation of PVA cryogels is also very remarkable. Even concentrated (10–16 wt%) aqueous and DMSO solutions of PVA (the latter must be highly deacylated PVA) do not transform to gels at room temperature for many days, whereas the freeze–thaw cycle produces viscoelastic cryogels that can be fused only when heated up to 60–80 °C. Similarly to the formation of chemically crosslinked cryogels, the main reason for such a decrease in CCG is the cryo-concentration of the gel precursors, strengthening the polymer–polymer interactions owing to higher overlapping of the polymer coils in the more concentrated medium of UFLMP.

## *3.2 Acceleration of Gel Formation Over a Certain Range of Negative Temperatures*

One of the important consequences of the cryo-concentration effect is an acceleration of cryotropic gel formation processes within a certain range of negative temperatures as compared with conventional gelation [8]. Since the rate of the second or higher order reactions is proportional to a positive power of the concentration of the reactants, a freezing-induced increase in the precursor concentration within the UFLMP accelerates cryogelation reactions [54, 62–64]. The reaction scheme in Fig. 10a illustrates the oxidative gelation of a thiol-derivative of poly (acrylamide) in the presence of water-dissolved air oxygen acting as a crosslinking agent [28, 153, 154]. Since the number of free SH groups decreases during the course of interchain coupling through the formation of disulfide crosslinks, the evolution of SH group concentration with time reflects the process dynamics. Figure 10b shows the variation in the amount of residual SH groups in 2 wt% aqueous polymer solutions at positive (15 and 25 °C) and negative (−15 and −25 °C) temperatures. Two arrows (Fig. 10b) indicate the vicinity of the gel points for the unfrozen and frozen gelation systems. The rate of the decrease in thiol group content (i.e., the crosslinking rate) increases and the gel point shifts to shorter times in the moderately frozen polymer solutions as compared to unfrozen solutions. Remarkable is the shortening of the gelation time, which differs by a factor of about 22 in favor of cryotropic gel formation.

The thermal prehistory of such cryogenically gelling systems also influences the process dynamics. The kinetic data in Fig. 10b were obtained by conventional freezing of the feeds, i.e., without low-temperature quenching, as mentioned in Sect. 2.2. When the same reaction solutions are subjected to the low-temperature quenching technique to freeze the feeds quickly, one obtains the plots illustrated in Fig.10c. Here, the decrease in the thiol group content of the polymer is shown during the course of the first 2 h of the reaction. Note that the zero time in these plots

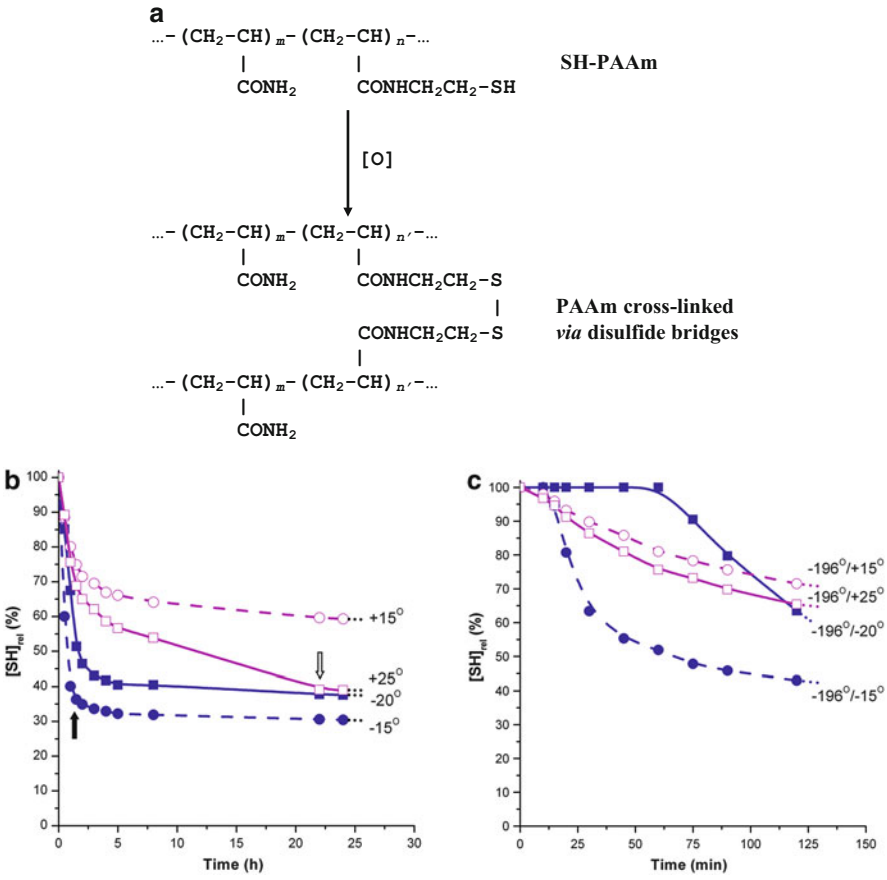


**Fig. 10** (**a**) Crosslinking reaction of thiol-containing poly(acrylamide) in aqueous acid solutions. (**b**, **c**) Variation in the percentage of residual thiol groups on the polymer chains with reaction time. The freezing technique was conventional (**b**) or low-temperature quenching (**c**). Gelation temperatures are indicated. *White* and *black arrows* in **b** indicate the vicinity of the gel points in unfrozen and frozen gelation systems, respectively. Plotted from the data of [28]

corresponds to the moment of transfer of the reaction solutions from liquid nitrogen into the cryostat/thermostat chamber with a pre-set temperature. A certain delay (i.e., lag period) is observable at the start of the reactions at negative temperatures, followed by a quick decline of the SH content of polymer chains. For the gelation reactions conducted at positive temperatures, the reaction rates with and without low-temperature quenching are identical. However, at negative temperatures, low-temperature quenching further accelerates the gelation reactions. Moreover, except for the lag phase, the slope of the kinetic curves obtained both at −15 and −20 °C is much higher than that obtained at positive temperatures. Thus, independent of the thermal history, the rate of the crosslinking reactions is much faster in frozen solutions than in unfrozen solutions due to the existence of UFLMP.

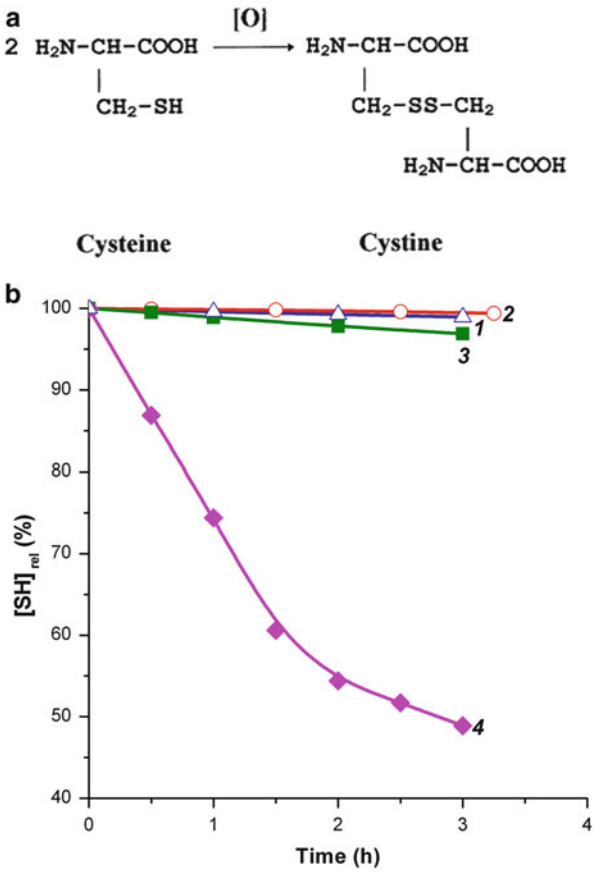


**Fig. 11** (**a**) Scheme of cysteine to cystine conversion. (**b**) Variation in the relative amount (%) of residual thiol groups on cysteine with reaction time for the reactions in the presence (*curves 2*, *4*) and absence of poly (acrylamide) (*curves 1*, *3*). Gelation temperature was −15 °C (*curves 3*, *4*) and +25°C (*curves 1*, *2*). (From [28] with permission from Elsevier)

The volume and concentration of solutes in UFLMP depend on the cryoscopic properties of the solvent, the freezing temperature, concentration of the precursors in the feed, their solubility, and their dimensions, i.e., molecular weights. In this connection, it is of interest to demonstrate how the presence of an inert additive (e.g., an inert polymer) can affect the reaction kinetics in such non-deeply frozen systems. This effect was investigated in cysteine–cystine conversion by oxygen [28]. Figure 11a shows the scheme of the oxidation of cysteine, a thiol-containing amino acid, to the respective disulfide by water-dissolved air oxygen. Figure 11b presents the kinetic curves of this reaction as the dependence of the thiol group content of cysteine on the reaction time [28]. When the reactions are conducted at room temperature or at −15 °C (represented by the curves 1 and 3, respectively, in Fig. 11b), the concentration of SH groups slowly diminishes with time due to this oxidation, i.e., the reactions proceed slowly. When the initial cysteine solution also contains about 1 wt% poly(acrylamide) as an inert polymeric additive, no marked effect was observed at room temperature (curve 2 in Fig. 11b). Thus, the polymer

does not have any chemical impact on the process of interest. However, a significant acceleration of cysteine oxidation occurs in the presence of polymer when the temperature is decreased to −15 °C (curve 4 in Fig. 11b). Since the water solubility of cysteine is low, the slow rate of the reactions in the frozen solution at −15 °C is due to the fact that the system is in the post-eutectic state and the amount of cysteine dissolved in UFLMP is very small. However, the presence of a hydrophilic unreactive polymer carrying bound water molecules increases the solubility of both cysteine and oxygen so that their concentrations in UFLMP increase and, hence, the reaction rate increases. This example also demonstrates one of the possible approaches for performing the reactions with thermally instable and insufficiently soluble low molecular weight substances. The presence of an inert polymeric additive during cryogelation protects the precursors from thermal decomposition and accelerates the reactions due to the cryo-concentration effect.

The acceleration of gel formation and the non-equivalence of its dynamics, depending on the thermal prehistory of moderately frozen reaction systems, were also observed during the synthesis of polymerization-type cryogels. One typical example is the formation of poly(acrylamide) gels starting from acrylamide monomer and *N*,*N*′-methylene(bis)acrylamide crosslinker in aqueous solutions with using of redox initiator systems (Fig. 12a). In Fig. 12b, c, gel fraction versus reaction time plots at various gelation temperatures are shown for reaction solutions frozen by conventional and low-temperature quenching procedures, respectively [23]. At positive temperatures, lowering the reaction temperature from 25 to 13 °C causes a decrease in the rate of ordinary gel formation, and thus results in a lower gel-fraction yield. This is expected. However, performing the reactions in a moderately frozen system leads to a faster gelation as well as to a higher yield (Fig. 12b). The freezing mode, i.e., the thermal history of bringing the system to the reaction temperature, also affects the course of cryotropic gel formation (cf. Fig. 12b, c), thus pointing to the non-equivalence of the phase states in such differently frozen polymerizing systems. Similar trends were also observed by use of NMR during the formation of poly(acrylamide) cryogels [50], as well as during the linear cryopolymerization of acrylamide in moderately frozen aqueous media, where different freezing procedures (conventional freezing, flash freezing, and low-temperature quenching) were employed [65].

The acceleration of gelation over a certain range of negative temperatures is also inherent during the formation of physical cryogels. This fact was already partially touched upon in the discussion of the data in Table 2, for instance, regarding the gelation time of aqueous solutions of locust bean gum or PVA. The same effect was also observed in maltodextin- and β-glucan-containing systems [101, 145, 146], i.e., in systems where the noncovalent self-gelation at positive temperatures proceeds at a rather slow rate. Probably, somewhat similar events do take place in fast-gelling systems such as aqueous solutions of agarose, amylopectin, amylopectin–amylose mixtures, or concentrated solutions of gelatin. However, because of their rapid self-gelation before freezing, the additional acceleration due to the presence of UFLMP can hardly be detected.

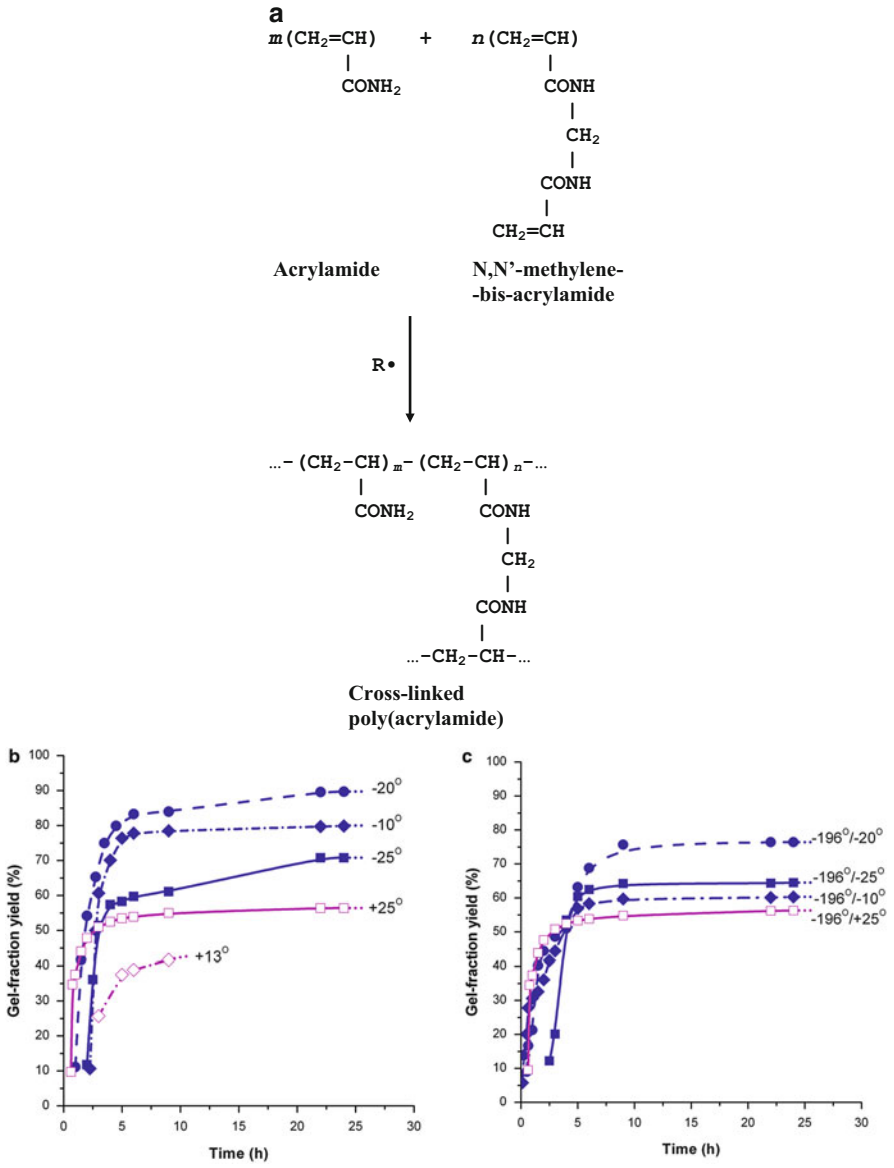


**Fig. 12** (**a**) Free-radical crosslinking copolymerization of acrylamide and *N*,*N*′-methylene(bis) acrylamide. (**b**, **c**) Gel-fraction yield plotted against reaction time for the case of conventional freezing (**b**) and low-temperature quenching (**c**). Gelation temperatures are indicated. (Plotted based on the data from [23])

### 3.3 Bell-Shaped Temperature Dependence of Cryotropic Gelation Efficiency

In early studies on the kinetic features of simple model reactions in moderately frozen systems, it was found that the temperature dependence of the reaction rates is bell-shaped [62, 63]. This type of temperature dependence is a consequence of competition between the acceleration effect because of the cryo-concentration and the deceleration effect due to the decreasing thermal mobility of the reactants and increasing viscosity in the medium of UFLMP at negative temperatures [54, 63]. The temperature dependence of cryotropic gelation efficiency is, as a rule, also bell-shaped during the formation of both covalent and noncovalent cryogels [8]. In the following, such effects are demonstrated for cryogels produced via chemical crosslinking of macromolecular precursors as well as for the polymerization-type and noncovalent cryogels.

Figure 13 shows the temperature dependence of the gel-fraction yield during the formation of chitosan-based cryogels, when this polyaminosaccharide was crosslinked with various amounts of glutaraldehyde (for the reaction scheme see Fig. 7a). The results reveal that, in the moderately frozen aqueous medium, the highest performance of the crosslinking process was achieved in the vicinity of −25 °C, whereas above and below this temperature the gel-fraction yield was lower [10].

Because the freezing procedure employed (i.e., the thermal history of the system) influences the cryotropic gelation dynamics, it is reasonable to anticipate that it can also affect the temperature dependence of the gel formation efficiency. Indeed, this assumption was confirmed experimentally. Figure 14 is a relevant example showing the temperature dependence of the initial rate ($v_0$) of SH group decline in the course of oxidative gelation of thiol-bearing poly(acrylamide) [28]. Curves 1 and 2 correspond to the reaction systems subjected to conventional freezing and low-temperature quenching procedures, respectively. The distinctions are obvious: when the reaction solution is subjected to the low-temperature quenching procedure, the initial rates become slower over the whole range of reaction temperatures studied, and the position of the maximum shifts towards a lower temperature. These results testify once again that the reaction conditions in moderately frozen systems, especially at the initial stages, differ significantly depending on the thermal prehistory, i.e., on the freezing procedure employed. Most probably, one of the main reasons for this effect is the nonequivalence of the phase states in such differently frozen gelling systems. Nonetheless, the bell-like character of curves 1 and 2 in Fig. 14 is very similar, thus showing the generality of the tendencies described by such temperature dependences, irrespective of the thermal history. At the same time, no differences were observed in $v_0$ values for the gelation in solutions without any freezing (solid line in Fig. 14) and initially frozen in a liquid nitrogen followed by placing in a thermostat with pre-set positive temperature (dashed line in Fig. 14).

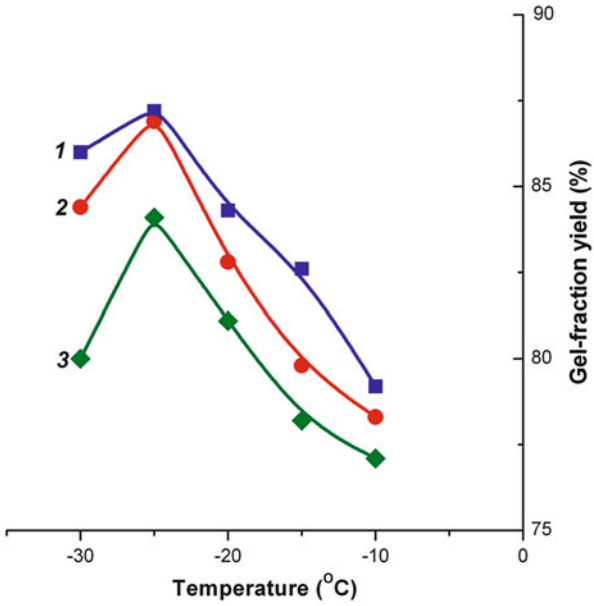


**Fig. 13** Gel-fraction yield plotted against temperature for chitosan cryogels crosslinked using glutaraldehyde. Polymer concentration in the initial solution was 1.6 wt%. $NH_2$-to-CHO molar ratio was 2.5:1 (*curve 1*), 15:1 (*curve 2*) and 25:1 (*curve 3*). (From [10] with permission from Springer)

The bell-shaped temperature dependence of the gelation rates is, as mentioned already, due to the competition between the favorable and adverse factors. The favorable factors are as follows:

1. The cryo-concentration effect leads to increased concentrations of solutes within the UFLMP, facilitating the reaction efficiency.
2. The effect of the so-called thermodynamic selection of the reactions [63] that are characterized by the lowest values of the activation energy.
3. The heat sink from the reaction system is useful for the exothermic processes so that it is also one of the favorable factors, provided that the heat is released during the gelation, as it usually is for free-radical polymerization.
4. Since the dielectric conductivity ε increases as the temperature decreases, the polarity of the solvent in UFLMP is higher than its polarity at positive temperatures, which is an additional favorable factor. For example, during the heterolytic reactions where the separation of charges is of significance, e.g., coupling of polymeric precursors through the formation of aldimine (Fig. 7a), alkyl-aryl (Fig. 8a), or acetal (Fig. 9a) crosslinks, increasing the polarity of the reaction medium also increases the efficiency of the respective reactions.
5. During the formation of noncovalent cryogels from the polymeric precursors exhibiting an upper-critical-solution-temperature (UCST) behavior, cooling down the reaction solution also facilitates the sol-to-gel transition.

There are also several factors acting adversely on gel formation in moderately frozen systems as follows:

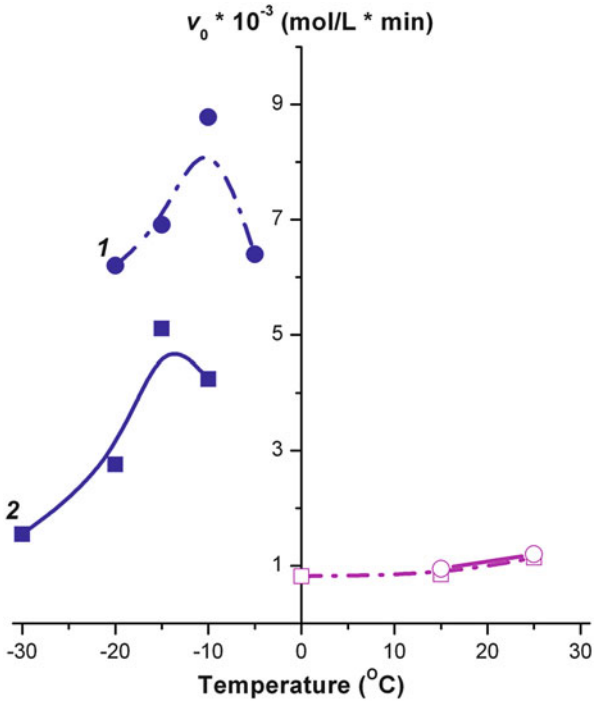


**Fig. 14** Initial rate $\nu_o$ of the decrease of thiol groups in aqueous solutions of thiol-containing poly (acrylamide) plotted against temperature. Freezing procedures were conventional (*curve 1*) and low-temperature quenching (*curve 2*). Polymer concentration in the initial solution was 2 g/L. (From [28] with permission from Elsevier)

1. According to the Arrhenius principle, a decrease in temperature lowers the thermal mobility of the solutes and thus, decelerates the reactions. This is the most significant unfavorable factor affecting the cryogelation process.
2. The high viscosity of UFLMP is the second unfavorable factor for cryotropic gel formation. This factor is significant for cryogelation reactions starting from polymeric precursors. Since the lower the temperature of a moderately frozen system, the larger the amount of frozen solvent and, thus, the higher the polymer concentration in UFLMP, the resulting high viscosity strongly hinders the translational and segmental mobilities of the polymeric precursors and interferes with their interactions. The molecular weight of the polymeric precursors also affects the course of gel formation. The higher the molecular weight of the polymeric solute, the higher is the extent of coil overlap and, hence, the higher is the probability of intermolecular interactions. On the other hand, the higher the chain length of the polymers, the higher is the viscosity of the equiconcentrated polymer solutions. Thus, these two trends act oppositely and compete against each other in the course of gel formation. This is also the reason why a bell-like dependence of the gelation efficiency on the molecular weight of the polymeric precursors is often observed. For particular examples, see [32, 44, 155] dealing with the synthesis of chitosan and poly(acrylamide) cryogels via crosslinking by glutaraldehyde, and with the noncovalent cryotropic gelation of aqueous

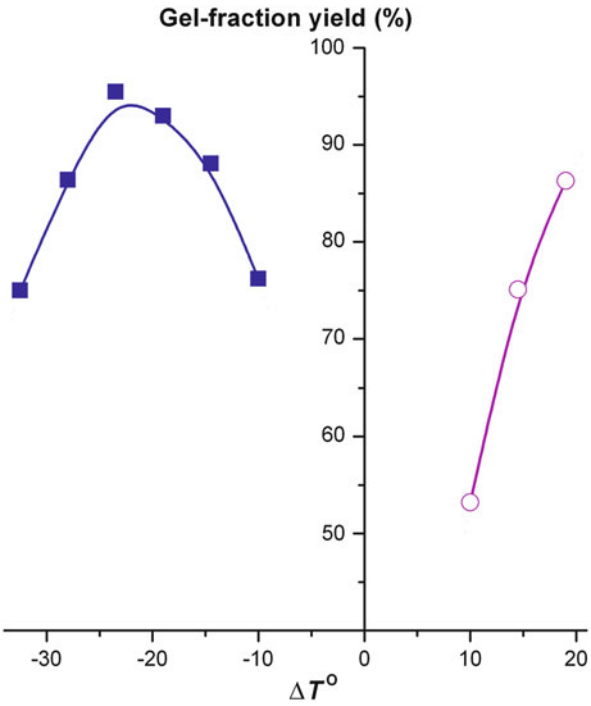


**Fig. 15** Temperature dependence of the gel-fraction yield during the preparation of poly(styrene) gels (*circles*) and cryogels (*squares*) in nitrobenzene using 4,4′-xylylene dichloride as a crosslinker. The temperature scale is the relative temperature $\Delta T$ (as explained in Sect. 1). Polymer and crosslinker concentrations in the initial nitrobenzene solution were 0.3 M and 9.1 mol%, respectively (both with respect to the styrene units). (Plotted based on the data from [27])

solutions of PVA of various molecular weights. Therefore, it is desirable to perform some preliminary experiments with polymeric precursors of different molecular weights in order to search for an optimum value of this parameter.

3. The formation rate of crosslinks between the polymer chains is also a factor capable of hindering the gelation processes inside the UFLMP. When the reactions proceed slowly, the crosslinks are generated rather uniformly throughout the UFLMP. However, for the fast reactions, the polymer chains are rapidly bridged by the introduction of the first crosslinks, once the primary network is formed, the subsequent crosslinks in highly viscous UFLMP are strongly hampered. This effect can result in a pronounced inhomogeneity in the crosslink density distribution within the network. To minimize this effect and, thus, to prepare cryogels with reproducible properties and porous morphology, one can reduce the reaction rates and the initial concentration of the precursors.

All these favorable and unfavorable factors and mechanisms are effective to a different extent during cryotropic gelation in both aqueous and organic media. For instance, Fig. 15 shows the bell-like temperature dependence of the gel-fraction yield when poly(styrene) was crosslinked with 4,4′-xylylene dichloride in nitrobenzene (see Fig.8a for the reaction scheme). At temperatures 30–40 °C lower than room temperature, the efficiency of polymer crosslinking is higher than in unfrozen solutions (curve with open circles in Fig. 15) [27]. Thus, close similarity in the character of such temperature dependences for the processes in frozen aqueous and

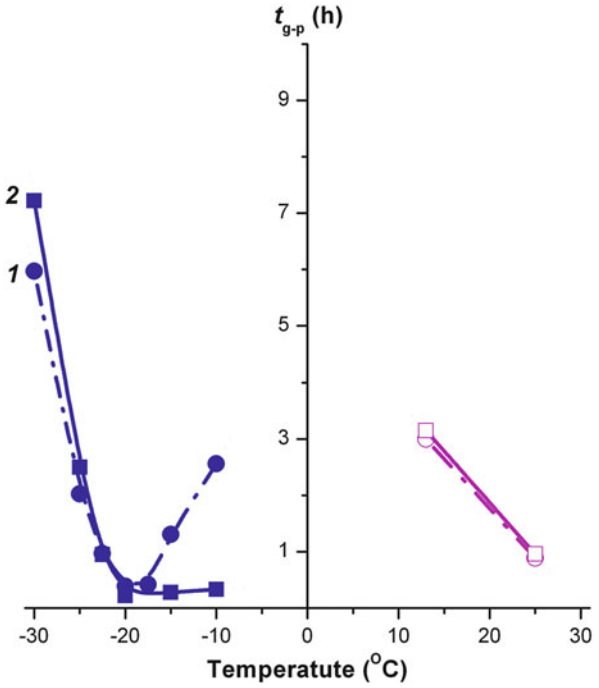


**Fig. 16** Time for the onset of gelation $t_{g-p}$ plotted against the temperature during the crosslinking copolymerization of acrylamide and *N*,*N*′-methylene(bis) acrylamide. Freezing modes were conventional freezing (*curve 1*) and low-temperature quenching (*curve 2*). Initial monomer concentration was 3 wt%. Molar ratio of vinyl to divinyl monomers in the feed was 30:1. (From [23] with permission from Wiley)

organic media obviously proves that the same factors are responsible for the efficiency of cryotropic gel formation in solvent–polymeric precursor–crosslinking agent systems, irrespective of the type of crystallizing solvent.

Temperature dependences of the rate of cryogelation reactions and the cryogel properties were also investigated in reaction systems leading to the formation of polymerization-type cryogels, i.e., in solvent–monomers–initiator systems. Figure 16 shows the reaction time for the onset of gelation (i.e., the gel-point time, $t_{g-p}$) during the redox-initiated copolymerization of acrylamide and *N*,*N*′′-methylene(bis)acrylamide in aqueous solutions plotted against the reaction temperature. The curves 1 and 2 in Fig. 16 represent the trend of data obtained from the reaction solutions subjected to conventional freezing and low-temperature quenching procedures, respectively [23]. The shortest time to reach the gel point at −20 °C was 15 and 14 min for the conventional freezing and low-temperature quenching, respectively. At room temperature, this time is about four times longer (~1 h). This feature was already touched on in the discussion on the acceleration effect inherent in cryotropic gelation as compared with gel formation at positive temperatures. Moreover, an interesting point can also be gained by comparing curves 1 and 2 in Fig. 16 within the temperature interval from −20 to −10 °C. For the reaction solution subjected to the conventional freezing procedure (curve 1), i.e., when the solution just after initiator addition is placed into the cryostat chamber with the required preset temperature, a concave upward bell-like dependence of $t_{g-p}$ on the reaction temperature was observed. In contrast, application of the

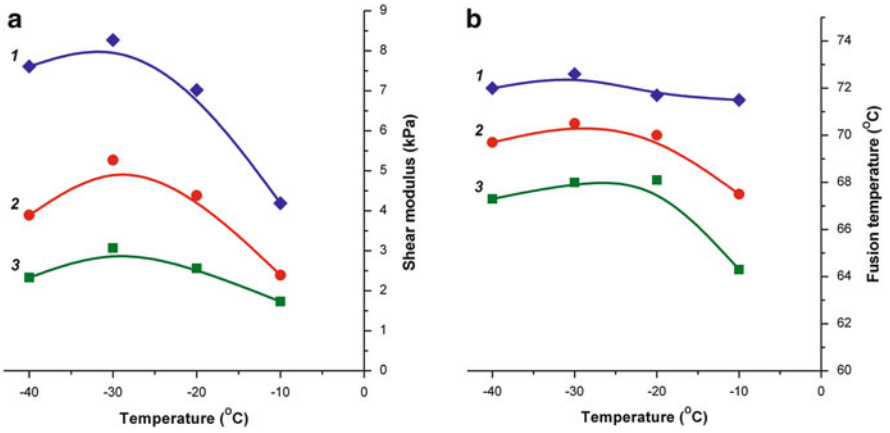


**Fig. 17** Influence of the freezing/frozen storage temperature on (**a**) the shear modulus and (**b**) the fusion temperature of PVA cryogels. Initial polymer concentrations were 120 (*curve 1*), 100 (*curve 2*), and 80 g/L (*curve 3*). (Plotted based on the data from [44])

low-temperature quenching procedure using liquid nitrogen markedly alters the temperature dependence between −10 and −20 °C. This result most probably indicates that, when a deeply frozen system is heated to the subzero level, the concentration of the reactants in the resulting UFLMP at the early stages of gel formation is higher than that in the UFLMP formed as a result of a conventional mode of freezing. The reason for such an effect is obviously a low rate of solid-to-liquid phase transition of solvent crystals after the low-temperature quenching [23, 50, 65]. This phenomenon in its nature resembles prolonged (days) thawing of snow and ice in spring when the environmental temperature is already considerably higher than the ice melting point.

The last example in this section concerns the temperature dependence of the efficiency of the noncovalent cryotropic gel formation. This is illustrated in Fig. 17 for PVA cryogels, where their shear moduli (Fig. 17a) and the fusion temperatures (Fig. 17b) are plotted as a function of the freezing temperature. The cryogels were prepared by freezing aqueous solutions of PVA (80–120 g/L) for a fixed time at various negative temperatures followed by defrosting at the same rate [44]. The modulus and the fusion temperature of the cryogels represent their rigidity and heat endurance, respectively, and are indicators of the gelation performance. It can be seen that both of these parameters also have bell-shaped dependences on the process temperature. This also indicates the competition of the facilitating and inhibiting mechanisms participating in the formation of such gel matrices. Thus, lowering the storage temperature of the frozen solution results in the formation of a larger mass of solvent crystals and, hence, increases the polymer concentration in UFLMP so that PVA gelation becomes more efficient, as in the case of systems having a higher initial PVA concentration in the feed. On the other hand, the drastic increase in viscosity within UFLMP hinders efficient intermolecular interactions

and, thus, formation of PVA microcrystallites, the nodes in the final cryogel. As a result, the temperature dependences of the respective parameters pass through the maxima, a common trend for the formation of physical cryogels in general.

Summing up the discussion on the influence of favorable and detrimental factors on cryotropic gel formation, one can see that their competition is the main reason for the bell-like temperature dependence of the gelation efficiency. This effect is manifested both for chemically crosslinked cryogels and noncovalent gels, when either monomeric or polymeric precursors are used, and both in aqueous and organic media. So, such bell-shaped dependences are a characteristic feature of cryotropic gel formation. However, the exact position of the corresponding maxima or minima on the temperature axis depends on the particular cryogelation system. Therefore, the necessity of preliminary search for the "optimal" temperature conditions for freezing and for frozen storage is evident. Although such preliminary studies can require time and effort, only this path will result in cryogels with the best possible properties and structure.

## *3.4 Generation of Specific Porosity Peculiar to Cryogels*

The scheme in Fig. 3 visually demonstrates formation of macroporosity in cryogels due to the presence of polycrystals of frozen solvent acting as porogens. Depending on the nature of the cryogel precursors, their initial concentrations, the type of the solvent used, and the cryogenic processing conditions, it is possible to obtain cryogels with pores having a cross-section from the submicron range up to several micrometers (Figs. 5 and 6), or supermacroporous (wide pore) gel matrices similar to the sponge-like chitosan-based cryogels (Fig. 1) where the cross-section of large pores ranges from tens to hundreds of micrometers. Certainly, some "intermediate" variants are also possible. The main characteristics of the porosity of cryogels have been described in several review papers [8, 9, 107, 111, 114, 130, 148–150, 152, 156–164], and are also considered in [47]. However, certain aspects of macroporosity generation in the course of freeze–thaw gelation will be discussed in this section.

We will first consider the reason why the size of pores in the cryogels varies by two orders of magnitude depending on the synthesis conditions. This is mainly due to the different size of the pore template (i.e., the frozen solvent polycrystals), which depends on the amount of freezable solvent under the freezing conditions employed. For instance, when the initial concentration of the monomeric precursors is not too high, i.e., less than 10 wt%, the fraction of free solvent freezable at moderate negative temperatures is large, and the viscosity of the feed solution is not so high as to markedly inhibit crystal growth. This effect leads to the formation of large polycrystals and, hence, large pores. On the other hand, when the initial concentration of the polymeric precursors is high, a greater part of the solvent is bound to the dissolved macromolecules so that the volume of the freezable liquid is considerably less than in the previous case, leading to a high solution viscosity that

hinders the growth of solvent crystals. As a result, only relatively small porogen particles can be formed, thus generating relatively small pores in the resulting cryogels.

In this connection, PVA solutions subjected to multiple freeze–thaw cycles represent a specific case where the porosity characteristics are governed not only by the conditions of the first cryogenic cycle, but also by the following cycles [111, 126–130, 133, 149, 165, 166]. As illustrated in Fig. 6, the most significant step-like changes in the size and shape of the macropores occur during the second cycle. During this cycle, the free solvent crystallizes mainly within the space of the already formed "primary" macropores, where the liquid contains only a small amount of sol-fraction [113]. Therefore, the viscosity within this space is considerably lower than that of the initial PVA solution, and larger ice particles are formed. In addition to widening of the primary pores by these growing crystals, a certain compression of the pore walls owing to the physical stresses caused by the ice crystallization also occurs, thus facilitating compaction of the proper gel phase in the heterophase material. As a consequence, after the second freeze–thaw cycle, the cross-section of the macropores increases by a factor of 2–3, whereas further cryogenic cycles have an insignificant influence on the size and shape of these pores [133].

The cryogenic processing conditions of PVA solutions also affect significantly the porous structure of PVA cryogels. To demonstrate this effect, noncovalent PVA cryogels were prepared starting from aqueous solutions of PVA (100 g/L) according to two different freezing and frozen-storage procedures [44]:

(a) PVA solution was frozen at −20 °C for 24 h
(b) PVA solution was first frozen at −20 °C for 1 h, then incubated at a fixed negative temperature between −5 and −1.1 °C for 23 h

The micrographs in Fig. 18a, b represent thin sections of PVA cryogels formed by the two procedures, respectively, where the latter was incubated at −2 °C. The morphology of the cryogel formed by a single-temperature freezing differs markedly from the two-temperature freezing procedure. As pointed out in Sect. 2.4, at a storage temperature of −2 °C, cryotropic gelation of PVA occurs with the highest efficiency. Moreover, ice re-crystallization phenomena are also very intensive at this temperature [167–169]. Since the prolonged incubation of the frozen sample at −2 °C equalizes the temperature fields in all directions, the branched crystals are formed as a result of the re-crystallization. After defrosting, such secondary crystals leave a net-like system of intersecting macropores in the body of the PVA cryogel.

The next key feature of the textural morphology of freeze–thaw gels is the interconnected character of their macropores. The main reason for such a porous character is the 3D growth of porogen particles (i.e., solvent crystals) during freezing of the feed system, whereby the growth stops for a particular facet of a crystal when it comes into tight contact with some facet of a neighboring growing crystal [8]. During subsequent thawing of the frozen sample, these contact areas are transformed into the connections between macropores. When the unidirectional freezing technique is employed, the propagation rates of different facets are

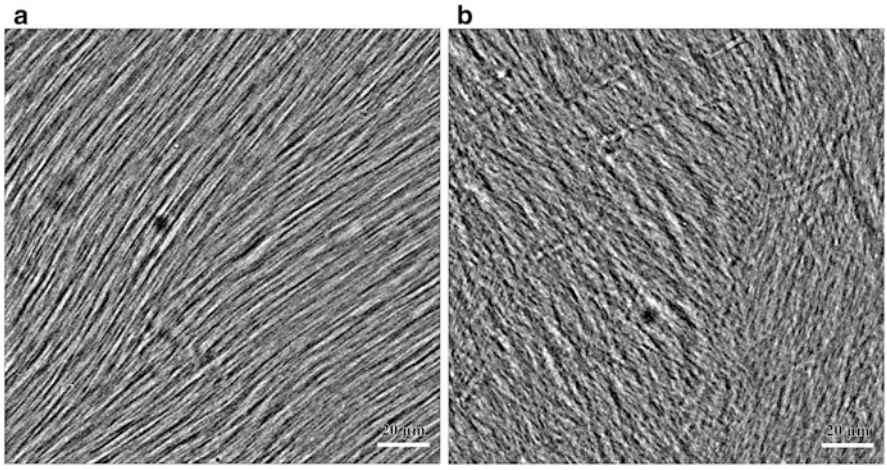


**Fig. 18** Micrographs of thin sections of PVA cryogels prepared from aqueous solutions of PVA (100 g/L) using (**a**) single-temperature and (**b**) two-temperature procedures. The freezing/storage-frozen regimes were −20 °C for 24 h (**a**) and −20 °C for 1 h and then −2 °C for 23 h (**b**). The average size of macropores was 2.8 (**a**) and 2.4 μm (**b**). The fraction of macropores was 61.3 (**a**) and 52.5 % (**b**). *Scale bars*: 20 μm. (From [44] with permission from Springer)

strongly unequal, and crystal growth dominates in the direction that follows the vector of temperature gradient. Nonetheless, other facets are also enlarged and have the possibility to come into contact with their neighbors, thus forming future connections between the unidirected macropores in the defrosted cryogel.

The interconnected character of the pores in stimuli-responsive cryogels is also responsible for their fast response rate to a change in the external conditions. As is well known [170, 171], hydrogels may exhibit drastic volume changes in response to specific external stimuli, such as temperature, solvent quality, pH, electric field, etc. However, such stimuli-responsive hydrogels prepared by conventional techniques exhibit a slow rate of response to external stimuli. For instance, the kinetics of the collapse of temperature-sensitive swollen hydrogels is controlled by heat transfer into the gel and by diffusion of the solvent out of the gel, where both of these processes depend on the size of the gel sample. The larger the gel size, the lower is its response rate. The presence of interconnected pores of capillary size in cryogels, as well as the high polymer content of their pore walls, ensure their very fast volumetric response to external stimuli. Thermoresponsive poly(*N*,*N*-diethylacrylamide) and poly(*N*-isopropylacrylamide) cryogels are typical examples of stimuli-responsive cryogels [172, 173]. As the temperature passes across the critical (LCST) point, the gel phase (pore walls) deswells so that the inner water is rapidly squeezed out of the cryogel through the system of interconnected capillaries. In such spongy gel matrices, absorption or desorption of water occurs through the macropores by convection, which is much faster than the diffusion process that dominates inside the conventional hydrogels. Figure 19 shows a typical example of the dynamics of heating-induced collapse of poly(*N*,*N*-diethylacrylamide) gels,

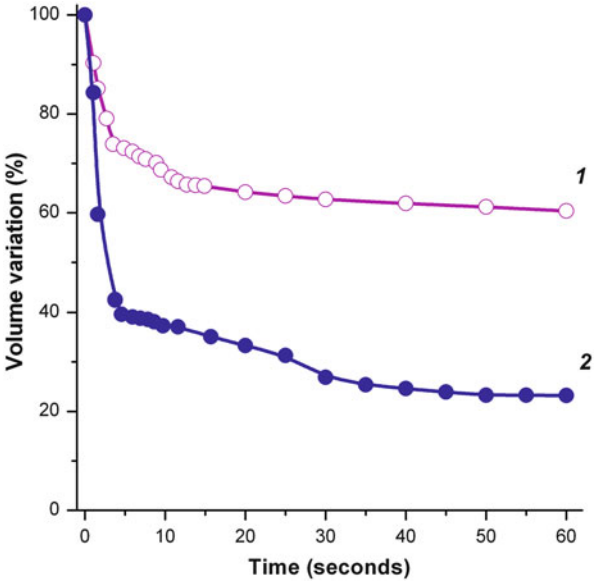


**Fig. 19** Thermally induced collapse of poly(*N*,*N*-diethylacrylamide) hydrogel (*curve 1*) and cryogel samples (*curve 2*) upon increasing the temperature from room temperature to 60 °C. The variation in the volume of the gel samples is shown as a function of the deswelling time. Synthesis conditions: initial monomer concentration 5.66 wt%; molar ratio of vinyl to divinyl monomers 200:1; gelation temperature +20 °C (*curve 1*) and −10°C (*curve 2*). (From [172] with permission from Springer)

where the variation in gel volume is plotted against the deswelling time. Here, the gel samples swollen to equilibrium in water at room temperature were immersed in water at 60 °C, and the volume change was recorded as a function of time. Data obtained from hydrogels and cryogels are shown in curves 1 and 2 of Fig. 19, respectively. Compared to the conventional gel, the rate of deswelling is much faster and the extent of volume variation is much larger for the cryogel sample due to its 3D pore structure.

Another aspect related to the formation of macroporous structure in polymeric cryogels is the implementation of auxiliary porogens in addition to the solvent crystals. Combination of various pore-forming agents allows one to vary the macroporous morphology of the cryogel-type materials over a very wide range. Such auxiliary agents can be divided into two groups: first, the pore-formers that can be later extracted from the gels, such as silica particles, salts, or oil droplets; and second, those that cannot, such as gas bubbles. In the first case, the corresponding porogens can be either temporarily insoluble or even soluble in the feed, while the second group includes permanently insoluble disperse matter playing the role of pores.

One of the simplest examples of a temporarily insoluble porogen is chalk or silica powder, whose particles are initially dispersed in the feed to be cryogenically

treated. Such feed systems result in the formation of composite cryogels with incorporated fillers, which are then dissolved by rinsing the composite with aqueous acid or alkali. The pores formed with the aid of such additives are isolated from each other and have a size close to that of the filler grains, whereas the system of interconnected macropores is ensured by cryotropic gel formation. Hydrophobic oil can also be used as an insoluble porogen in the preparation of hydrophilic thermo- or pH-responsive poly(*N*-isopropylacrylamide)-based copolymer cryogels [174–176]. After preparation of such wide-pore spongy gel composites, they contain entrapped microdroplets of hydrophobic liquid. These droplets can be removed upon the stimulus-induced collapse of the cryogel, i.e., by heating or by changing pH. Since the collapse is reversible, when the collapsed cryogel is placed in oil-free water, it swells again so that additional "non-cryotropic" spherical pores filled with water instead of oil microdroplets can be obtained. By iterative collapse–swelling cycles it is possible to remove completely such hydrophobic auxiliary porogens.

The soluble auxiliary pore-forming agents are compounds dissolved in the common solvent together with the gel precursors. The porogenic properties of these agents may affect the crystallization of the liquid medium so that they are also called modifiers of solvent crystals. This effect is illustrated by the micrographs in Fig. 20, which show the images of thin sections of PVA cryogels prepared in the presence of various low molecular weight salts at two different concentrations. All the samples were cryostructured under identical freeze–thaw conditions, and Table 3 summarizes their porosity parameters [177]. The porous morphology of PVA cryogels is affected by both the nature and the concentration of low molecular weight electrolyte additives. The size of the macropores decreases as the salt concentration is increased, in accord with the well-known influence of salts on the spatial geometry and size of ice crystals [167, 178, 179]. Moreover, the influence of other processes like the salting-out effect, which leads to an increase in the ionic strength of UFLMP, cannot be excluded. As a result, certain integral changes in the macroporous morphology of cryogels can be registered at the resolution provided by an optical microscope. In other words, such low molecular weight salt additives act as powerful pore modifiers for the resulting cryogels, and their impact is achieved via their influence on the course of solvent crystallization.

Certain soluble auxiliary pore forming agents may induce a liquid–liquid phase separation. Spongy PVA-based cryogels prepared from "water–PVA–gum arabic" feeds are a good example of the influence of such phenomenon on the formation of additional pores in cryogels [180]. Aqueous feed systems containing a gel-forming agent (PVA) and a polymeric additive (gum arabic) unable to form noncovalent cryogels are interesting because they demonstrate the effect of thermodynamic incompatibility of the polymeric components on the texture of the resulting cryogels. Several types of PVA cryogels prepared from such multicomponent feeds have been described, where the auxiliary pore-forming agents were both synthetic polymers and natural biopolymers such as polysaccharides, proteins, and nucleic acids. All of these additives affect the properties and the porous structure of the formed PVA cryogels [181–187]. There are potentially two extreme variants of PVA-based feed systems capable of liquid-phase de-mixing. First, the

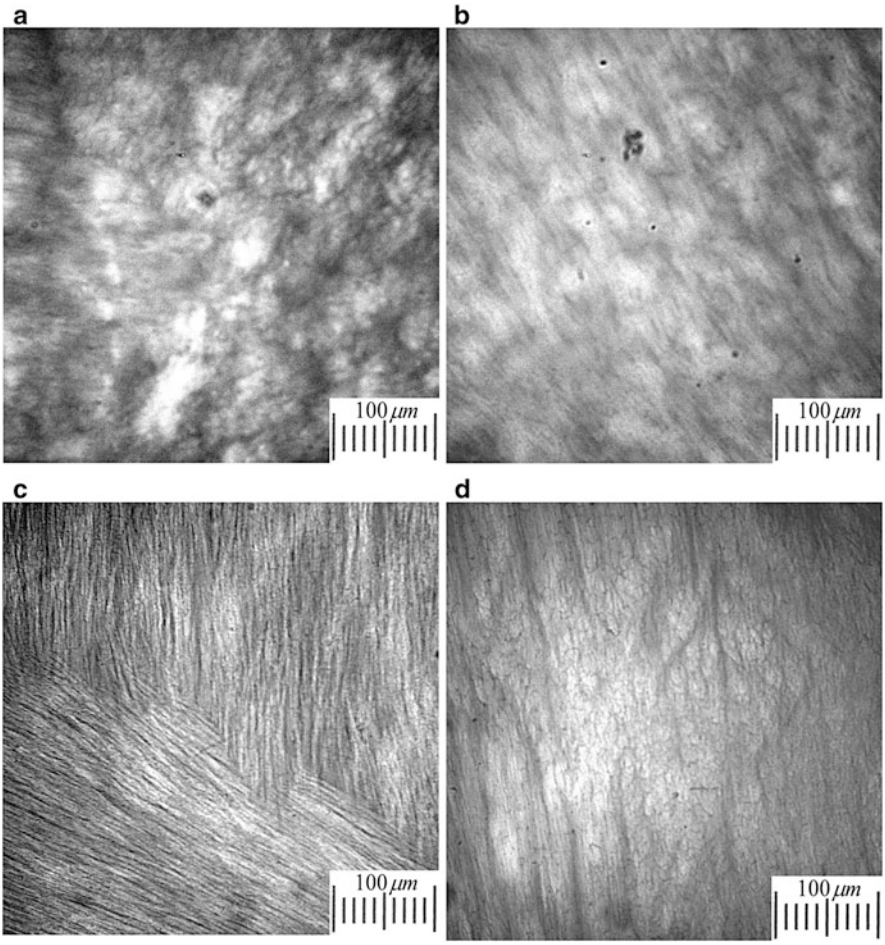


**Fig. 20** (continued)

solution of PVA and the polymer additive can be frozen while in a homophase liquid state. As the pure ice is initially crystallized, both polymeric components are concentrated in the UFLMP. This cryo-concentration process causes liquid–liquid phase separation within the volume of the unfrozen inclusions. In the second case, the initial common solution of PVA and the polymeric additive can undergo liquid–liquid separation prior to the cryogenic treatment, a behavior inherent in the well-known Albertsson's liquid two-phase polymeric systems [188], so that the already formed two coexisting liquids are frozen. Certainly, there can be some intermediate variants because the phase segregation in viscous polymer solutions occurs rather slowly, i.e., the process is kinetically controlled.

An example of the first case is the preparation of macroporous PVA cryogels in aqueous solutions of PVA in the presence of poly(ethylene glycol) of molecular

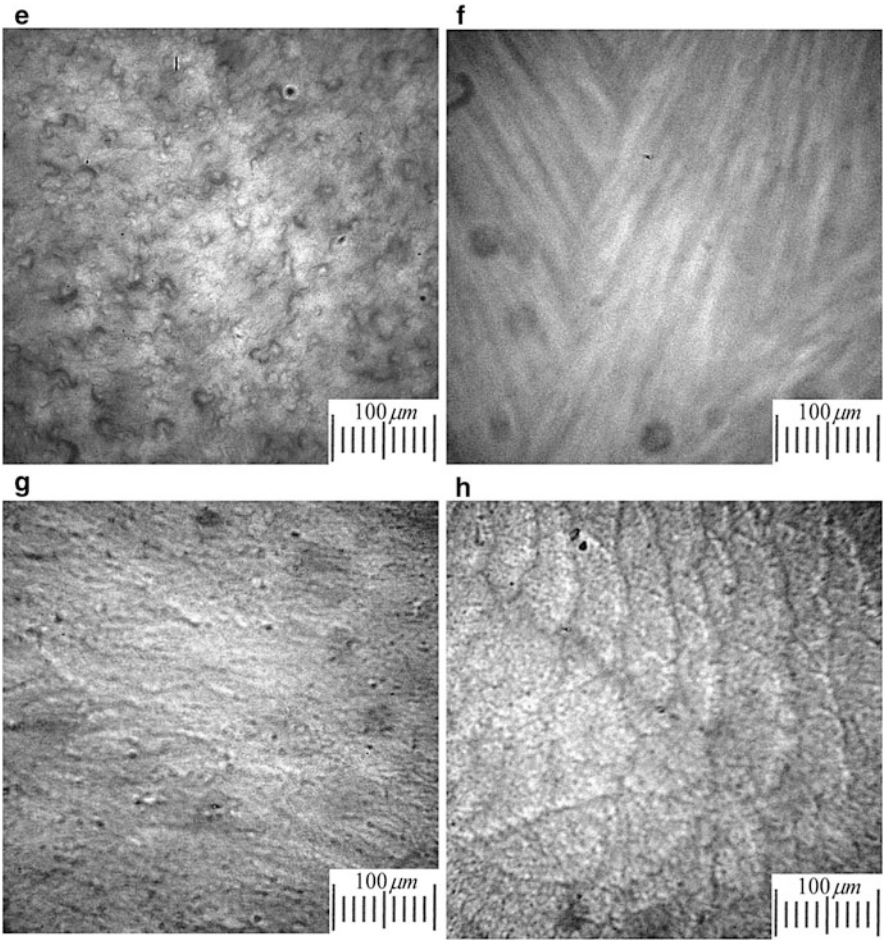


**Fig. 20** (**a**–**h**) Micrographs of thin sections of PVA cryogels formed in the presence of alkali metal chloride additives at a concentration of 0.6 (**a**, **b**, **c**, **d**) and 1.2 M (**e**, **f**, **g**, **h**). Salt additives: LiCl (**a**, **e**), NaCl (**b**, **f**), KCl (**c**, **g**), and CsCl (**d**, **h**). Initial polymer concentration was 100 g/L. Conditions of cryotropic gelation were freezing at −20°C for 24 h and defrosting with a rate of 0.03 °C/min. (From [177] with permission from Springer)

weight 1,000 g/mol (PEG-1000) acting as an auxiliary porogen [182]. At PEG-1000 concentrations below 10 wt%, although the initial solution is homophase, two liquid phases appear within the UFLMP during the course of the freezing/frozen-storage stage due to the freeze-induced concentrating effect. NMR studies show that these are PVA-rich and PEG-rich phases [151, 189]. Cryotropic gelation of the PVA-rich phase fixes the morphology of the complex system containing segregated phases. Thus, the PEG-rich phase acts as the auxiliary porogen causing the formation of so-called "compartments" [189], i.e., the large pores in addition to the ice-templated pores.

**Table 3** Data from morphometric analysis of images of thin sections of PVA cryogels formed without and with salt additives

| Alkali metal chloride | Salt concentration in the initial solution (M) | Morphometric data | |
|---|---|---|---|
| | | Fraction of macropores (%) | Average size of macropores (μm) |
| – | 0 | 57.7 | 5.62 |
| LiCl | 0.3 | 61.6 | 4.73 |
| | 0.6 | 63.8 | 3.02 |
| | 0.9 | 53.8 | 2.74 |
| | 1.2 | 46.9 | 2.51 |
| NaCl | 0.3 | 42.0 | 2.40 |
| | 0.6 | 55.4 | 2.32 |
| | 0.9 | 76.6 | 2.14 |
| | 1.2 | 48.6 | 2.11 |
| KCl | 0.3 | 50.1 | 2.77 |
| | 0.6 | 57.6 | 3.03 |
| | 0.9 | 64.4 | 2.62 |
| | 1.2 | 52.7 | 2.58 |
| CsCl | 0.3 | 47.0 | 2.29 |
| | 0.6 | 54.4 | 2.79 |
| | 0.9 | 52.1 | 2.77 |
| | 1.2 | 55.1 | 2.81 |

From [177] with permission from Springer

Another type of auxiliary extractable porogen is gum arabic (GuAr), which was used for the preparation of PVA cryogels from the above-mentioned two-phase ternary system, namely from the "water–PVA–GuAr" system. This system contains the gel-forming PVA and the water-soluble GuAr, whose aqueous solutions per se are not transformed into cryogels after freezing–frozen storage–thawing stages. The cryotropic gelation of such feeds at various PVA/GuAr ratios and concentrations, as well as the properties of the resulting gel matrices were explored in detail in the study [180]. The micrographs in Fig. 21 demonstrate the hierarchy of the macropores in such cryogels. Here, the morphology of the cryogel samples is given at four different magnifications. The dark areas in the pictures are the PVA-based gel phase stained with Congo Red, while the clear areas are the pores of various shape and size. The gross through-hole pores with a cross-section of the order of 1 mm can be observed, even in the survey photograph of a whole 2-mm-thick disc (Fig. 21a). These capillary-sized pores are also seen in an optical microscope at a low magnification (Fig. 21b). At a fivefold higher resolution (Fig. 21c), one can distinguish a high porous morphology of the gel matter, which is the continuous phase in this spongy heterogeneous material, where the roundish pores are also observed. The micrograph in Fig. 21d of the thin section illustrates the structure of space between the gross pores. Here, at least two kinds of pores are distinguished within these gel matrices, namely the "larger" roundish pores of 10–70 μm in diameter (some of which are somewhat deformed) and the "smaller" pores, also rounded, of ~1–5 μm in diameter. Hence, these micrographs

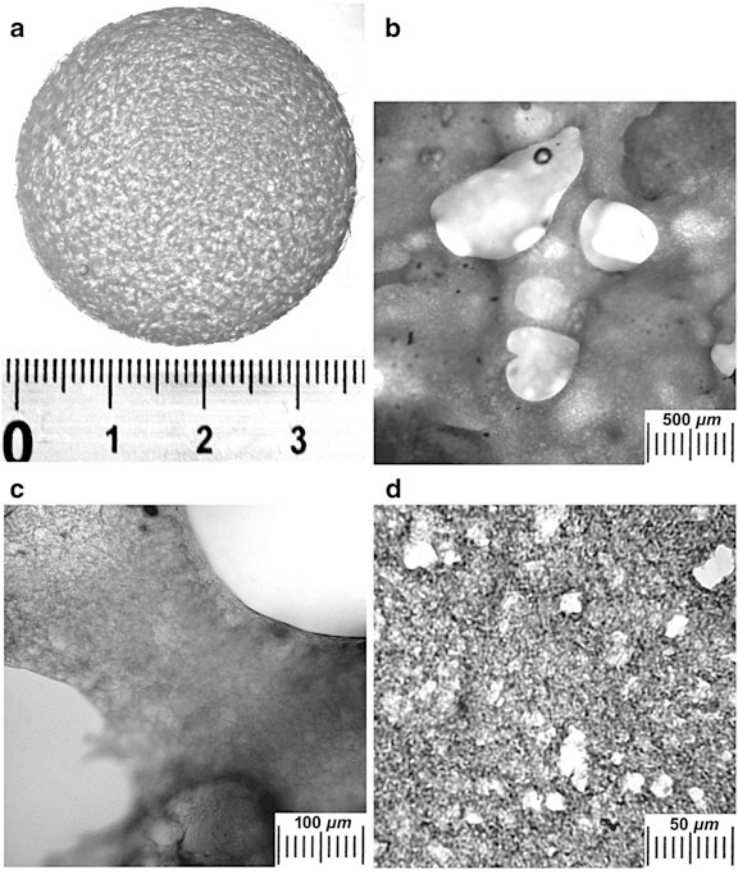


**Fig. 21** Porous morphology of wide-pore PVA cryogels prepared using the feed system water–PVA–GuAr. (**a**) Photograph of 2-mm-thick disc stained with Congo Red. (**b**, **c**) Survey micrographs of the same disc obtained with an optical microscope at two different magnifications. (**d**) The image of a thin section of the disc. (From [180] with permission from RCS)

testify to the definite hierarchy in the porous morphology of such polymeric gels prepared by combining the processes of liquid–liquid phase separation and cryotropic gelation.

Note that the fine microstructure of such gel systems is provided by the light microscopy of their thin sections, a technique successfully employed for the analysis of various PVA cryogels, including conventional, complex, and composite gels [44, 48, 133, 150, 177, 190]. This technique is important because it allows visualization of the intact morphology of water-swollen PVA cryogels, whereas, for instance, SEM analysis allows the observation of either dried or frozen (cryo-SEM) samples that are not intact.

The hierarchical pore system of the cryogels under discussion is manifested in the presence of several kinds of macropores that differ significantly in their size.

Whereas the largest capillary pores are interconnected and, therefore, liquids can easily leak through blocks of such wide-pore cryogels (Fig. 21a, b), the rounded pores of other kinds are closed (Fig. 21c, d). The former are replicas of the continuous GuAr-rich phase in the two-phase system formed as a result of liquid–liquid separation. The heterogeneous morphology of such a system is fixed by the cryotropic gelation of the PVA-rich phase. Since the cross-section of pores in conventional PVA cryogels generated by the ice polycrystals does not usually exceed 1–3 μm [92, 95, 126, 150, 165, 166, 177, 191], it is evident that the 10–70-μm pores (Fig. 21b, d) are also replicas of the non-gelling GuAr-rich phase, but in this case dispersed as liquid droplets in the bulk PVA-rich phase. Moreover, the smallest pores visible in the light microscopy image of Fig. 21d are, most probably, left in the gel matter by the ice particles after thawing. The pores of the latter type have a rounded shape, whereas those observed in the "conventional" PVA cryogels prepared under the same conditions but without foreign polymeric additives are usually anisodiametric (prolate) in their shape (see Figs. 5, 6, and 18). We have to mention that the round-shaped ice-derived pores in PVA cryogels are also inherent in the gel matrices prepared with the addition of surfactants as pore modifiers, which are capable of influencing the shape of the ice crystals by decreasing the surface tension at the solid–liquid interface during crystal growth [192]. Thus, such "rounding" of the pores inside the gel phase of wide-pore cryogels fabricated from the water–PVA–GuAr feeds are probably due to the surfactant properties of GuAr macromolecules present in a small amount in the initial PVA-rich phase.

The last type of auxiliary pore-forming agents that will be considered here are the gaseous porogens. These agents are constantly being entrapped in the cryogel matrix and perform as the pores per se. Examples of such porogens are small gas bubbles, and the resulting gas-filled cryogels can be termed "foamed cryogels." Inside the foamed freeze–thaw gels, two sorts of macropores can be distinguished: the cryogenically induced macropores, i.e., those derived from the thawed solvent polycrystals, and the closed microbubbles remaining entrapped in the cryogel after defrosting of the frozen foam. Such gas-filled gel materials, PVA-based gels in particular, have been prepared, studied, and some promising instances of their practical application have been reported [192–197]. In these works, the gaseous porogen was generated either using physical methods, e.g., whipping, barbotage, microfluidic foaming techniques [192–194, 197], or via the chemical liberation of gas products, e.g., by the reaction of ammonium chloride with sodium nitrite ($NH_4Cl + NaNO_2 \rightarrow NaCl + 2H_2O + N_2\uparrow$), that were introduced into the feed prior to its freezing [196].

For instance, foamed cryogels were fabricated by mechanical whipping of aqueous PVA solutions followed by freezing of the resulting foams, storing the samples frozen, and then slowly defrosting [193]. The peculiarities of the porous morphology of such gel foamed matrices are illustrated by the microphotographs in Fig. 22a, b, which show thin sections of the samples prepared by cryostructuring of the PVA-based liquid foam. These foamed cryogels possess two sorts of pores distinguishable by optical light microscopy. The first type are the gross round pores of ~50 to ~250 μm in diameter formed by the auxiliary pore-forming agent, i.e., by

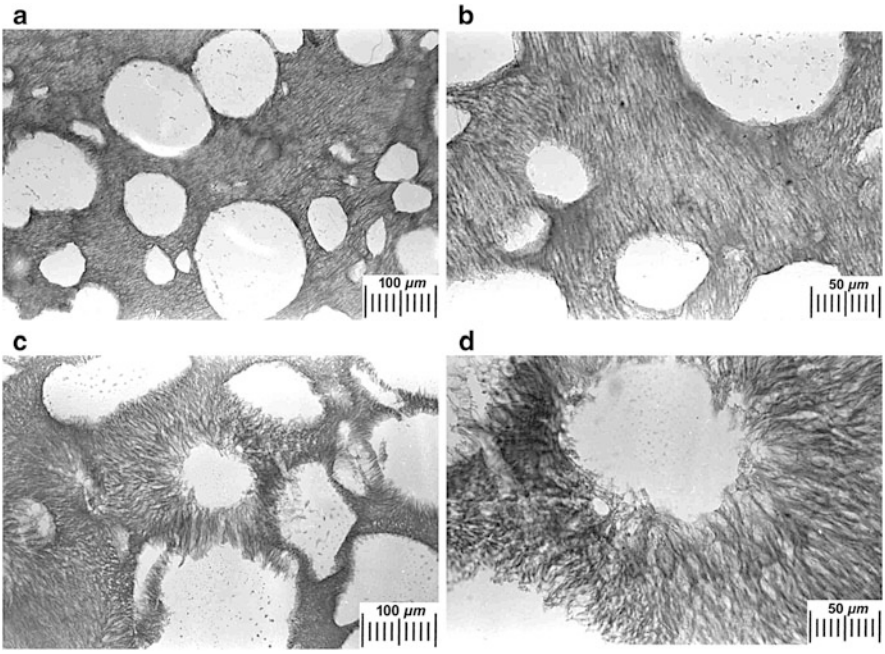


**Fig. 22** Optical micrographs at two different magnifications of thin sections of foamed PVA cryogels prepared from the fluid foam produced by whipping of aqueous polymer solutions in the (**a**, **b**) absence and (**c**, **d**) presence of the surfactant CTAB at a concentration of 0.415 mM. Initial polymer concentration was 120 g/L. Cryotropic gelation conditions: freezing temperature −20 °C; freezing duration 18 h, thawing rate 0.03 °C/min. (From [192] with permission from Springer)

the air bubbles. The second type are smaller prolate pores with a cross-section of around 1–3 μm within the gel phase in the space between the bubbles. The pores of the latter type are typical of cryogenically induced pores in conventional PVA cryogels (e.g., see Figs. 5 and 6), and these pores are filled with water rather than gas. The microbubble-type pores generated by simple whipping or by the barbotage of a gas through a porous filter to the initial polymer solution have a wide size distribution. In this respect, a recently developed microfluidic foaming technique is attractive because it allows a rather narrow, practically monodisperse distribution of pore dimensions [197]. The air bubbles entrapped in the PVA cryogel matrix decrease its density down to values smaller than that of water, thus imparting buoyancy to such cryogels, i.e., foamed cryogels can float in water for a long time and do not sink [193].

The impact of surfactant additives on the porous structure of foamed cryogels is of special interest. Fig. 22c, d shows the micrographs, at two different magnifications, of thin sections of foamed PVA cryogels stained with Congo Red. The gel samples were prepared by whipping of an aqueous PVA solution having the same initial polymer concentration as the sample shown in Fig. 22a, b, but it additionally contained dissolved surfactant, cetyltrimethylammonium bromide (CTAB). Even

at a small concentration of CTAB (e.g., 0.415 mM), the microstructure of the cryogel undergoes very significant changes [192]. The cross-section of the ice-templated pores is enlarged from 1–3 μm (Fig. 22b) to 4–5 μm (Fig. 22d) due to the presence of the ionic surfactant. Simultaneously, the morphology of the gel–gas interfaces also changes drastically. Although the surface of these interfaces in surfactant-free foamed cryogel is almost smooth (Fig. 22a, b), the presence of CTAB causes pronounced ulceration of the surface (Fig. 22c, d). A similar effect was also observed using sodium dodecyl sulfate as an anionic surfactant additive [192]. Thus, the presence of surfactants significantly affects the shape of the gaseous macropores. It is evident that bubbles with such a pitted surface cannot exist in the initial liquid foam, since such foam would be absolutely unstable. Therefore, this unusual morphology of the gas–gel interfaces appears to be due to the decreased surface tension between the liquid–gas interfaces and the growing facets of ice crystals, which can evidently pierce the air bubbles. However, the freezing solidification of the foam and consequent formation of cryogel in the bubble walls prevent the complete destruction of the bubbles, thus "imprinting" a certain intermediate structure of the boundary layers. Hence, surfactants similar to CTAB in terms of their influence on the foams can be considered as auxiliary modifiers of the architecture of gaseous pores within the foamed cryogels.

The results presented here thus show that there are very broad possibilities for affecting the macroporosity parameters in diverse cryogels and to govern, within certain limits, the architecture and size of the pores templated by the solvent crystals. In addition, there are many possibilities for creating multifarious additional macropores in these gel matrices by using auxiliary porogens. In each particular case, the approach employed depends on the purpose of the produced cryogel and on the set of material properties required for its efficient application.

## 4 Conclusions

Finalizing the overview of the literature related to the general aspects of cryotropic gelation processes, the following basic conclusions can be drawn [7–9, 105, 107, 111, 114, 148]:

1. Cryotropic gel formation is a liquid-phase process occurring in the unfrozen liquid microphase of a macroscopically frozen system.
2. The final products of such cryostructuring are macroporous, sometimes wide-pore sponge-like, gel matrices, i.e., cryogels.
3. Due to concentrating of solutes in the unfrozen liquid microphase, an apparent decrease in the critical concentration of gelation is observed in cryotropic gel formation as compared to gelation at positive temperatures
4. Acceleration of the gel formation is usually observed in the moderately frozen systems over a definite range of negative temperatures. The key reason for such

an acceleration is also the increased concentration of gel precursors in the unfrozen liquid microphase compared with their concentration in the initial feed.
5. A bell-like dependence of the gelation efficiency on the process temperature is inherent in cryotropic gel formation.
6. The properties and macroporous morphology of cryogels are controlled by the gelation temperature, solvent used, concentration of the gelling compounds, the presence of other solutes, freezing and thawing rates, freezing mode, duration of the frozen storage, and some other factors.

Finally, polymeric cryogels have a wide range of applications; this statement is confirmed by the majority of recent experimental papers and reviews relating to the implementation of cryogel-type materials in various applied areas (e.g., see reviews [152, 163, 164, 198–203] published in 2013). Certain important aspects related to the application of various cryogels are also considered in the subsequent chapters of the present volume.

**Acknowledgements** The work was supported by the joint Russian–Turkish grant from the Russian Foundation for Basic Research (Project # 12-03-91371-CT-a) and the Scientific and Technical Research Council of Turkey (Project # 211 T044). The authors also thank Drs. Andrey Ryabev and Roman Ivanov for the valuable help in the artwork preparation.

## References

1. Lozinsky VI (2014) A brief history of polymeric cryogels. In: Okay O (ed) Polymeric cryogels: macroporous gels with remarkable properties. Advances in Polymer Science, vol 263. Springer, Heidelberg
2. Papkov SP (1974) Gel-like state of polymers. Khimiya, Moscow, in Russian
3. Kudela V (1987) Encyclopedia of polymer science and engineering, vol. 7. Wiley, New York, p 783
4. Tanaka T (1987) In: Nicolini C (ed) Structure and dynamics of biopolymers. Dordrecht: M. Nijhoff, p 237
5. Rogovina LZ, Vasil'ev VG, Braudo EE (2008) Polym Sci 50C:85
6. Nishinari K (2009) Prog Colloid Polym Sci 136:87
7. Lozinsky VI (1994) DSc Thesis, Institute of Organoelement Compounds, Russian Academy of Sciences. Moscow, in Russian
8. Lozinsky VI (2002) Russ Chem Revs 71:489
9. Lozinsky VI, Plieva FM, Galaev IY, Mattiasson B (2001) Bioseparation 10:163
10. Nikonorov VV, Ivanov RV, Kil'deeva NR, Bulatnikova LN, Lozinsky VI (2010) Polym Sci 52A:828
11. Lozinsky VI, Vainerman ES, Rogozhin SV (1982) SU Patent 1,008,214
12. Rogozhin SV, Lozinsky VI, Vainerman ES, Domotenko LV, Mamtsis AM, Ivanova SA, Shtil'man MI, Korshak VV (1984) Doklady Akademii nauk SSSR 278:129–133, in Russian
13. Labudzińska A, Ziabicki A (1971) Koll Z u Z Polym 243:21
14. Schulze WE, Yu DT, MacMaters MM (1964) Stärke 16:41
15. Schierbaum F, Richter M (1964) Nahrung 8:487, in German
16. Blažek L, Dvoržak E, Myšik S (1964) Koll Zhurn 26:657, in Russian
17. Neiman RE (1967) Coagulation of synthetic latexes. Voronezh State University, Voronezh, pp 148–159, in Russian

18. Jellinek HHG, Fok SY (1967) Makromol Chem 104:18
19. Lozinsky VI, Korneeva MN, Vainerman ES, Rogozhin SV (1983) Doklady Akademii nauk SSSR 270:101, in Russian
20. Lozinsky VI, Vainerman ES, Titova EF, Belavtseva EM, Rogozhin SV (1984) Colloid Polym Sci 262:769
21. Belavtseva EM, Titova EF, Lozinsky VI, Vainerman ES, Rogozhin SV (1984) Colloid Polym Sci 262:775–779
22. Lozinsky VI, Vainerman ES, Ivanova SA, Titova EF, Shtil'man MI, Belavtseva EM, Rogozhin SV (1986) Acta Polym 37:142
23. Lozinsky VI, Morozova SA, Vainerman ES, Titova EF, Shtil'man MI, Belavtseva EM, Rogozhin SV (1989) Acta Polym 40:8
24. Ozmen MM, Okay O (2008) React Funct Polym 68:1467
25. Ozmen MM, Dinu MV, Okay O (2008) Polym Bull 60:169
26. Lozinsky VI, Vainerman ES, Rogozhin SV (1982) Colloid Polym Sci 260:776
27. Lozinsky VI, Vainerman ES, Korotaeva GF, Rogozhin SV (1984) Colloid Polym Sci 262:617
28. Lozinsky VI, Golovina TO, Gusev DG (2000) Polymer 41:35
29. Ivanov RV, Lozinsky VI, Noh SK, Han SS, Lyoo WS (2007) J Appl Polym Sci 106:1470
30. Tuncaboylu DC, Okay O (2009) Eur Polym J 45:2033
31. Orakdogen N, Karacan P, Okay O (2011) React Funct Polym 71:782
32. Nikonorov VV, Ivanov RV, Kil'deeva NR, Lozinsky VI (2011) Polym Sci 53A:1150
33. Bloch K, Lozinsky VI, Galaev IY, Yavriyanz K, Vorobeychik M, Azarov D, Damshkaln LG, Mattiasson D, Vardi P (2005) J Biomed Mater Res 75A:802
34. Lozinsky VI, Damshkaln LG, Bloch KO, Vardi P, Grinberg NV, Burova TV, Grinberg VY (2008) J Appl Polym Sci 108:3046
35. Flink JM, Johansen A (1985) Biotechnol Lett 7(10):765
36. Johansen A, Flink JM (1986) Biotechnol Lett 8(2):121
37. Vainerman ES, Lozinsky VI, Rogozhin SV, Raskina LP, Shapiro LA, Yakubovich VS, Bronshtein VY (1983) SU Patent 1:171,474
38. Vainerman ES, Lozinsky VI, Rogozhin SV, Raskina LP, Shapiro LA, Yakubovich VS, Shenker MB, Komissarova AL, Potapov VD, Gudochkova VM, Atyasova NM, Ivanova GA (1983) SU Patent 1,171,476
39. Zhang H, Cooper AI (2007) Adv Mater 19:1529
40. Gutiérrez MC, Ferrer ML, del Monte F (2008) Chem Mater 20:634
41. Franks F (1981) In: Morris GJ, Clarke A (eds) Effects of low temperatures on biological membranes. Academic, New York 3
42. Luyet BJ (1966) In: Meryman HT (ed) Cryobiology. Academic, New York, 115
43. Libbrecht KG (2005) Rep Prog Phys 68:855
44. Lozinsky VI, Damshkaln LG, Shaskol'skii BL, Babushkina TA, Kurochkin IN, Kurochkin II (2007) Colloid J 69:747
45. Tuncaboylu DC, Okay O (2010) Langmuir 26:7574
46. Ak F, Oztoprak Z, Karakutuk I, Okay O (2013) Biomacromolecules 14:719
47. Okay O, Lozinsky VI (2014) Synthesis and structure–property relationships of cryogels. In: Okay O (ed) Polymeric cryogels: macroporous gels with remarkable properties. Advances in polymer science, vol 263. Springer, Heidelberg
48. Lozinsky VI, Damshkaln LG, Kurochkin IN, Kurochkin II (2012) Colloid J 74:319
49. Ivanov RV, Lozinsky VI (2006) Polym Sci 48A:1232
50. Gusev DG, Lozinsky VI, Bakhmutov VI (1993) Eur Polym J 29:49
51. Vonnegut B, Chessin H (1971) Science 174:945
52. Kirsebom H, Rata G, Topgaard D, Mattiasson B, Galaev IY (2008) Polymer 49:3855
53. Zheng L, Sun DW (2006) Trends Food Sci Technol 17:16
54. Sergeev GB, Batyuk VA, Stepanov MB, Sergeev BM (1973) Doklady Akademii nauk SSSR 213:891, in Russian
55. Grant NH, Clark DE, Alburn HE (1961) J Am Chem Soc 83:4476

56. Grant NH, Clark DE, Alburn HE (1962) J Am Chem Soc 84:876
57. Butler AR, Bruice TC (1964) J Am Chem Soc 86:313
58. Bruice TC, Butler AR (1964) J Am Chem Soc 86:4104
59. Pincock RE, Kiovsky TE (1965) J Am Chem Soc 87:2072
60. Grant NH, Clark DE, Alburn HE (1966) J Am Chem Soc 88:4071
61. Pincock RE, Kiovsky TE (1966) J Chem Educ 43:358
62. Pincock RE (1969) Acc Chem Res 2:97
63. Sergeev GB, Batyuk VA (1976) Russ Chem Rev 45:391
64. Batyuk VA (1987) The chemistry of low temperatures and cryochemical technology. Moscow State University, Moscow, p 163, in Russian
65. Ivanov RV, Babushkina TA, Lozinsky VI (2005) Polymer Sci 47A:791
66. Kuntz ID (1971) J Am Chem Soc 93:514
67. Kvlividze VI, Pylova MB (1977) Kolloidn zhurn 39:1167, in Russian
68. Katayama S, Fujiwara S (1980) J Phys Chem 84:2320
69. Suzuki E, Nagashima N (1982) Bull Chem Soc Jpn 55:2730
70. Ogino K, Sato H (1995) J Polym Sci Polym Phys 33:445
71. Masuda K, Horii F (1998) Macromolecules 31:5810
72. Martin DR, Ablett S, Darke A, Sutton RL, Sahagian M (1999) J Food Sci 64:46
73. Mil' EM, Kovarskii AL, Vasserman AM (1973) Izv AN SSSR Ser khim 10:2211, in Russian
74. Mikhalev OI, Yakovleva IV, Trofimov VI, Shapiro AB (1985) Cryo Lett 6:245
75. Mikhalev OI, Karpov IN, Kazarova EB, Alfimov MV (1989) Chem Phys Lett 164:96
76. Mikhalev OI, Serpinski M, Lozinsky VI, Kapanin PV, Chkeidze II, Alfimov MV (1991) Cryo Lett 12:197
77. Smith P, Pennings AJ (1974) Polymer 15:413
78. Gusev DG, Lozinsky VI, Vainerman ES, Bakhmutov VI (1990) Magn Reson Chem 28:651
79. Ricciardi R, Auriemma F, Gaillet C, De Rosa C, Lauprêtre F (2004) Macromolecules 37:9510
80. Kaetsu I (1993) Adv Polym Sci 105:81
81. Zhang XZ, Zhuo RX (1999) Macromol Rapid Commun 20:229
82. Kumakura M (2001) Polym Adv Technol 12:415
83. Yao K, Shen S, Yun J, Wang L, He X, Yu X (2006) Chem Eng Sci 61:6701
84. Plieva FM, Galaev IY, Mattiasson B (2007) J Sep Sci 30:1657
85. Reichelt S, Abe C, Hainich S, Knolle W, Decker U, Prager A, Konieczny R (2013) Soft Matter 9:2484
86. Lozinsky VI, Golovina TO, Vainerman ES, Rogozhin SV (1989) Polym Sci USSR 31A:367
87. Petrov P, Petrova E, Tchorbanov B, Tsvetanov CB, Reiss G (2007) Polymer 48:4943
88. Liu X, Hu Y, Zou J, Chai, Li B (2013) Appl Mech Mater 295–298:1368
89. Watase M, Nishinari K, Nambu M (1983) Polym Commun 24:52
90. Watase M, Nishinari K (1983) Polym Commun 24:270
91. Watase M, Nishinari K, Ogino K, Nambu M (1983) Polym Commun 24:345
92. Lozinsky VI, Vainerman ES, Domotenko LV, Mamtsis AM, Titova EF, Belavtseva EM, Rogozhin SV (1986) Colloid Polym Sci 264:19
93. Domotenko LV, Lozinsky VI, Vainerman ES, Rogozhin SV (1988) Polym Sci USSR 30A:1758
94. Lozinsky VI, Domotenko LV, Vainerman ES, Rogozhin SV (1989) Polym Sci USSR 31A:1983
95. Lozinsky VI, Vainerman ES, Domotenko LV, Blumenfel'd AL, Rogov VV, Barkovskaya EN, Fedin EI, Rogozhin SV (1989) Colloid J USSR 51:592
96. Konstantinova NR, Lozinsky VI (1997) Food Hydrocolloids 11:113
97. Damshkaln LG, Simenel IA, Lozinsky VI (1999) J Appl Polym Sci 74:1978
98. Lozinsky VI, Damshkaln LG, Brown CRT, Norton IT (2000) J Appl Polym Sci 75:1740
99. Lozinsky VI, Damshkaln LG (2000) J Appl Polym Sci 77:2017
100. Lozinsky VI, Damshkaln IG, Brown R, Norton IT (2000) Polym Int 49:1434
101. Lozinsky VI, Damshkaln LG, Brown CRT, Norton IT (2002) J Appl Polym Sci 83:1658

102. Zeira A, Nussinovich A (2004) J Texture Stud 34:561
103. Elowsson L, Kirsebom H, Carmignac V, Durbeej M, Mattiasson B (2012) J Mater Sci Mater Med 23:2489
104. Lozinsky VI, Ivanov RV, Kalinina EV, Timofeeva GI, Khokhlov AR (2001) Macromol Rapid Commun 22:1441
105. Lozinsky VI, Ivanov RV (2003) In: Monakov YB (ed) Synthesis and modification of polymers. Khimiya, Moscow, p 68, in Russian
106. Zaborina OE, Buzin MI, Lozinsky VI (2012) Polym Sci 54B:354
107. Lozinsky VI, Galaev IY, Plieva FM, Savina IN, Jungvid H, Mattiasson B (2003) Trends Biotechnol 21:445
108. Ferrero C, Martino MN, Zaritzky NE (1993) Int J Food Sci Technol 17:191
109. Lozinsky VI, Damshkaln LG, Brown R, Norton IT (2000) J Appl Polym Sci 78:371
110. Hyon SH, Cha WI, Ikada Y (1989) Kobunshi Ronbunshu 46:673, in Japanese
111. Lozinsky VI (1998) Russ Chem Rev 67:573
112. Lozinsky VI, Plieva FM (1998) Enzyme Microb Technol 23:227
113. Lozinsky VI, Zubov AL, Savina IN, Plieva FM (2000) J Appl Polym Sci 77:1822
114. Lozinsky VI (2008) Russ Chem Bull 57:1015
115. Tanaka R, Hatakeyama T, Hatakeyama H (1998) Polym Int 45:118
116. Matusevich LN (1968) Crystallization from solutions in chemical industry. Khimiya, Moscow, p 304, in Russian
117. Hassan CM, Ward JH, Peppas NA (2000) Polymer 41:6729
118. Ricciardi R, Gaillet C, Ducouret G, Lafuma F, Laupretre F (2003) Polymer 44:3375
119. Ricciardi R, Auriemma F, Rosa CD, Laupretre F (2004) Macromolecules 37:1921
120. Valentín JL, López D, Hernández R, Mijangos C, Saalwächter K (2009) Macromolecules 42:263
121. Watase M, Nishinari K, Nambu M (1983) Cryo Lett 4:197
122. Watase M (1983) Nippon Kagaku Kaisi 7:973, in Japanese
123. Nagura M, Nagura M, Ishikawa H (1984) Polym Commun 25:313
124. Watase M, Nishinari K (1985) Makromol Chem 186:1081
125. Watase M, Nishinari K (1985) J Polym Sci Polym Phys 23:1803
126. Yokoyama F, Masada I, Shimamura K, Ikawa T, Monobe K (1986) Colloid Polym Sci 264:595
127. Nambu M (1990) Kobunshi Ronbunshu 47:695, in Japanese
128. Urushizaki F, Yamaguchi H, Nakamura K, Namajiri S, Sugibayashi K, Morimoto Y (1990) Int J Pharm 58:135
129. Peppas NA, Stauffer SR (1991) J Control Release 16:305
130. Hassan CM, Peppas NA (2000) Adv Polym Sci 153:37
131. Wan WK, Campbell G, Zhang ZF, Hui AJ, Boughner DR (2002) J Biomed Mater Res 63:854
132. Sweeszkowski W, Ku DN, Bersee HEN, Kurzcydlowski KJ (2006) Biomaterials 27:1536
133. Lozinsky VI, Damshkaln LG, Kurochkin IN, Kurochkin II (2008) Colloid J 70:189
134. Roberts JD, Caserio MC (1977) Basic principles of organic chemistry, 2nd edn. W.A. Benjamin, Menlo Park
135. Horkay F, Nagy M (1981) Acta Chim Acad Sci Hung 107:321
136. Peppas NA (1987) In: Peppas NA (ed) Hydrogels in biology and medicine II. CRC, Boca Raton, p 1
137. Davis BJ (1964) Ann NY Acad Sci 121:404
138. Sun K, Sehon AH (1965) Can J Chem 43:969
139. Righetti PG, Brost BSW, Snyder RS (1981) J Biochem Biophys Methods 4:347
140. Maier H, Anderson M, Karl C, Magnuson K, Whistler RL (1993) In: Whistler RL, BeMiller JN (eds) Industrial gums. Academic, San Diego, p 181
141. Richardson PH, Clark AH, Russell AL, Aymard P, Norton IT (1999) Macromolecules 32:1519
142. Dea ICM, Morris ER, Rees DA, Welsh J, Barnes HA, Price J (1977) Carbohydr Res 57:249

143. Dea ICM (1987) In: Yalpani M (ed) Industrial polysaccharides: genetic engineering, structure/property relations and applications. Elsevier, Amsterdam, p 207
144. Bringham JE, Gidley MJ, Hoffmann RA, Smith CG (1994) Food Hydrocolloid 8:331
145. Lazaridou A, Biliaderis CG, Izydorczyk MS (2003) Food Hydrocolloid 17:693
146. Lazaridou A, Biliaderis CG (2004) Food Hydrocolloid 18:933
147. Richter M, Augustat S, Schierbaum F (1969) Ausgewahlte Metoden Der Starkechemie. VEB Fachbuchverlag, Leipzig, in German
148. Lozinsky VI, Vakula AV, Zubov AL (1992) Soviet Biotechnol #4:1
149. Gutiérrez MC, Aranaz I, Ferrer ML, del Monto F (2010) Production and properties of poly (vinyl alcohol) cryogels: recent developments. In: Mattiasson B, Kumar A, Galaev I (eds) Macroporous polymers: production, properties and biological/biomedical applications. CRC, Boca Raton, p 83
150. Alves MH, Jensen BEB, Smith AAA, Zelikin AN (2011) Macromol Biosci 11:1293
151. Shapiro YE (2011) Prog Polym Sci 36:1184
152. Gun'ko VM, Savina IN, Mikhalovsky SV (2013) Adv Colloid Interface Sci 186/187:1
153. Vainerman ES, Lozinsky VI, Rogozhin SV (1981) Colloid Polym Sci 259:1198–1201
154. Lozinsky VI, Golovina TO, Vainerman ES, Rogozhin SV (1989) Polym Sci USSR 31A:367
155. Ivanov RV, Lozinsky VI, Noh SK, Lee YR, Han SS, Lyoo WS (2008) J Appl Polym Sci 107:382
156. Dainiak MB, Galaev IY, Kumar A, Plieva FM, Mattiasson B (2007) Adv Biochem Eng Biotechnol 106:101
157. Plieva FM, Galaev IY, Noppe W, Mattiasson B (2008) Trends Microbiol 16:543
158. Kumar A, Mishra R, Reinwald Y, Bhat S (2010) Mater Today 13:42
159. Okay O (2010) Production of macroporous polymeric materials by phase separation polymerization. In: Mattiasson B, Kumar A, Galaev I (eds) Macroporous polymers: production, properties and biological/biomedical applications. CRC, Boca Raton, p 3
160. Plieva FM, Galaev IY, Mattiasson B (2010) Production and properties of cryogels by radical polymerization. In: Mattiasson B, Kumar A, Galaev I (eds) Macroporous polymers: production, properties and biological/biomedical applications. CRC, Boca Raton, p 23
161. Kirsebom H, Mattiasson B (2011) Polym Chem 2:1059
162. Plieva FM, Kirsebom H, Mattiasson B (2011) J Sep Sci 34:2164
163. Henderson TMA, Ladewig K, Haylock DN, McLean KM, O'Connor AJ (2013) J Mater Chem B 1:2682
164. Zhang H, Zhang F, Wu J (2013) React Funct Polym 73:923
165. Trieu HH, Qutubuddin S (1995) Polymer 36:2531
166. Willcox PJ, Howie DW, Schmidt-Rohr K, Hoagland DA, Gido S, Pudjijanto S, Kleiner LW, Venkatraman S (1999) J Polym Sci Polym Phys 37:3438
167. Franks F (ed) (1982) Water and aqueous solutions at subzero temperatures. New York, Plenum
168. Regand A, Goff HD (2003) Food Hydrocolloid 17:95
169. Libbrecht KG (2005) Reports Prog Phys 68:855
170. Ward MA, Georgiu TK (2011) Polymers 3:1215
171. Doring A, Birnbaum W, Kuckling D (2013) Chem Soc Rev 42:7391
172. Lozinsky VI, Kalinina EV, Grinberg VY, Grinberg NV, Chupov VA, Platé NA (1997) Polym Sci 39A:1300
173. Zhang XZ, Zhuo RX (1999) Macromol Chem Phys 200:2602
174. Komarova GA, Starodubtsev SG, Lozinsky VI, Kalinina EV, Landfester K, Khokhlov AR (2008) Langmuir 24:4467
175. Komarova GA, Starodubtsev SG, Lozinsky VI, Nasimova IR, Khokhlov AR (2013) J Appl Polym Sci 127:2703
176. Komarova GA, Starodubtsev SG, Khokhlov AR (2013) Polym Sci 55A:415
177. Lozinsky VI, Sakhno NG, Damshkaln LG, Bakeeva IV, Zubov VP, Kurochkin IN, Kurochkin II (2011) Colloid J 73:234

178. Finnegan WG, Pitter RL (1997) J Colloid Interface Sci 189:322
179. Wang S, Amornwittawat N, Banatlao J, Chung M, Kao Y, Wen X (2009) J Phys Chem 113B:13891
180. Lozinsky VI, Damshkaln LG, Ezernitskaya MG, Glotova YK, Antonov YA (2012) Soft Matter 8:8493
181. Suzuki M, Hirasa O (1993) Adv Polym Sci 110:241
182. Lozinsky VI, Solodova EV, Zubov AL, Simenel IA (1995) J Appl Polym Sci 58:171
183. Cascone MG, Maltini S, Barbani, Laus M (1999) J Mater Sci Mater Med 10:431
184. Cascone MG, Barbani N, Maltini S, Lazzeri L (2001) Polym Int 50:1241
185. Bajpai A, Saini R (2005) Polym Int 54:796
186. Mathews DT, Birney YA, Cahill PA, McGuinness CB (2008) J Appl Polym Sci 109:1129
187. Bajpai A, Saini R (2009) J Mater Sci Mater Med 20:2063
188. Albertsson PA (1971) Partition of cell particles and macromolecules, 2nd edn. Wiley-Interscience, New York
189. Shapiro YE, Shapiro TI (1999) J Colloid Interface Sci 217:322
190. Savina IN, Lozinsky VI (2004) Colloid J 66:343
191. Trieu HH, Qutubuddin S (1964) Colloid Polym Sci 272:301
192. Lozinsky VI, Damshkaln LG, Kurochkin IN, Kurochkin II (2005) Colloid J 67:589
193. Lozinsky VI, Damshkaln LG (2001) J Appl Polym Sci 82:1609
194. Altunina LK, Manzhai BN, Fufaeva MS (2006) Russ J Appl Chem 79:1669
195. Altunina LK, Kuvshinov VA, Dolgikh SN (2006) In: Lombardi S, Altunina LK, Beaubien SE (eds) Advances in the geological storage of carbon dioxide. NATO Science Series IV: earth and environmental sciences, vol. 65. Springer, Netherlands, p.103
196. Altunina LK, Manzhai BN, Stas'eva LA, Fufaeva MS (2007) Russ J Appl Chem 80:1647
197. Colosi C, Costantini M, Barbetta A, Pecci R, Bedini R, Dentini M (2013) Langmuir 29:82
198. Iatridis JC, Nicoll SB, Michalek AJ, Walter BA, Gupta MS (2013) Spine J 13:243
199. Barroso T, Hussain A, Roque ACA, Aguiar-Ricardo A (2013) Biotechnol J 8:671
200. Pfaunmiller EL, Paulemond ML, Dupper CM, Hage DS (2013) Anal Bioanal Chem 405:2133
201. Sheldon RA, van Pelt S (2013) Chem Soc Rev 42:6223
202. Kharkar PM, Kiick KL, Kloxin AM (2013) Chem Soc Rev 42:7335
203. Tanthapanichakoon W, Tamon H, Nakasawa K, Charinpanitkul T (2013) Eng J 17:1